ADSORPTION, GAS SEPARATION

1. Introduction

Gas-phase adsorption is widely employed for the large-scale purification or bulk separation of air, natural gas, chemicals, and petrochemicals (Table 1). In these

Table 1. **Commercial Adsorption Separations**

Separation[a]	Adsorbent
gas bulk separations	
normal paraffins, isoparaffins, aromatics	zeolite
N_2/O_2	zeolite
O_2/N_2	carbon molecular sieve
CO, CH_4, CO_2, N_2, Ar, NH_3/H_2	zeolite, activated carbon
acetone/vent streams	activated carbon
C_2H_4/vent streams	activated carbon
H_2O/ethanol	zeolite
gas purifications	
H_2O/olefin-containing cracked gas, natural gas, air, synthesis gas, etc.	silica, alumina, zeolite
CO_2/C_2H_4, natural gas, etc.	zeolite
organics/vent streams	activated carbon, others
sulfur compounds/natural gas, hydrogen, liquefied petroleum gas (LPG), etc.	zeolite
solvents/air	activated carbon
odors/air	activated carbon
NO_x/N_2	zeolite
SO_2/vent streams	zeolite
Hg/chlor–alkali cell gas effluent	zeolite

[a] Ref. 1.

uses, it is often a preferred alternative to the older unit operations of distillation and absorption.

An adsorbent attracts molecules from the gas, the molecules become concentrated on the surface of the adsorbent, and are removed from the gas phase. Many process concepts have been developed to allow the efficient contact of feed gas mixtures with adsorbents to carry out desired separations and to allow efficient regeneration of the adsorbent for subsequent reuse. In nonregenerative applications, the adsorbent is used only once and is not regenerated.

Most commercial adsorbents for gas-phase applications are employed in the form of pellets, beads, or other granular shapes, typically $\sim$1.5–3.2 mm in diameter. Most commonly, these adsorbents are packed into fixed beds through which the gaseous feed mixtures are passed. Normally, the process is conducted in a cyclic manner. When the capacity of the bed is exhausted, the feed flow is stopped to terminate the loading step of the process, the bed is treated to remove the adsorbed molecules in a separate regeneration step, and the cycle is then repeated.

The growth in both variety and scale of gas-phase adsorption separation processes, particularly since 1970, is due in part to continuing discoveries of new, porous, high-surface area adsorbent materials (particularly molecular sieve zeolites) and, especially, to improvements in the design and modification of adsorbents. These advances have encouraged parallel inventions of new process concepts. Increasingly, the development of new applications requires close cooperation in adsorbent design and process cycle development and optimization.

2. Adsorption Principles

The design and manufacture of adsorbents for specific applications involves manipulation of the structure and chemistry of the adsorbent to provide greater attractive forces for one molecule compared to another, or, by adjusting the size of the pores, to control access to the adsorbent surface on the basis of molecular size. Adsorbent manufacturers have developed many technologies for these manipulations, but they are considered proprietary and are not openly communicated. Nevertheless, the broad principles are well known.

This article is focused on physical adsorption, which involves relatively weak intermolecular forces, because most commercial applications of adsorption rely on this phenomenon alone. Chemisorption is discussed only briefly in some sections on specific applications.

2.1. Adsorption Forces. Coulomb's law allows calculations of the electrostatic potential resulting from a charge distribution, and of the potential energy of interaction between different charge distributions. Various elaborate computations are possible to calculate the potential energy of interaction between point charges, distributed charges, etc. See (2) for a detailed introduction.

An electric dipole consists of two equal and opposite charges separated by a distance. All molecules contain atoms composed of positively charged nuclei and negatively charged electrons. When a molecule is placed in an electric field between two charged plates, the field attracts the positive nuclei toward the negative plate and the electrons toward the positive plate. This electrical distortion, or polarization of the molecule, creates an electric dipole. When the field is removed, the distortion disappears, and the molecule reverts to its original condition. This electrical distortion of the molecule is called induced polarization; the dipole formed is an induced dipole.

The magnitude of the induced dipole moment depends on the electric field strength in accord with the relationship $\mu_i = \alpha F$, where μ_i is the induced dipole moment, F is the electric field strength, and the constant α is called the polarizability of the molecule. The polarizability is related to the dielectric constant of the substance. Group-contribution methods (2) can be used to estimate the polarizability from knowledge of the number of each type of bond within the molecule, eg, the polarizability of an unsaturated bond is greater than that of a saturated bond.

The total potential energy of adsorption interaction may be subdivided into parts representing contributions of the different types of interactions between adsorbed molecules and adsorbents. Adopting the terminology of Barrer and Vaughan (3), the total energy Φ_{Total} of interaction is the sum of contributions resulting from dispersion energy Φ_D, close-range repulsion Φ_R, polarization energy Φ_P, field–dipole interaction $\Phi_{F-\mu}$, field gradient–quadrupole interaction $\Phi_{\delta F-Q}$, and adsorbate–adsorbate interactions, denoted self-potential Φ_{SP}:

$$\Phi_{\text{Total}} = \underbrace{\Phi_D + \Phi_R + \Phi_P}_{\text{nonspecific}} + \underbrace{\Phi_{F-\mu} + \Phi_{\delta F-Q}}_{\text{specific}} + \underbrace{\Phi_{\text{SP}}}_{\text{adsorbate-adsorbent}}$$

The Φ_D and Φ_R terms always contribute, regardless of the specific electric charge distributions in the adsorbate molecules, which is why they are called

nonspecific. The third nonspecific Φ_P term also always contributes, whether or not the adsorbate molecules have permanent dipoles or quadrupoles; however, for adsorbent surfaces that are relatively nonpolar, the polarization energy Φ_P is small.

The $\Phi_{F-\mu}$ and $\Phi_{\delta F-Q}$ terms are specific contributions, which are significant when adsorbate molecules possess permanent dipole and quadrupole moments. In the absence of these moments, these terms are zero, as is true also if the adsorbent surface has no electric fields, a completely nonpolar adsorbent.

Finally, the Φ_{SP} term is the contribution resulting from interactions between adsorbate molecules. At low coverages of the adsorbent by adsorbate molecules, this contribution approaches zero, and at high coverage it often causes a noticeable increase in the heat of adsorption.

The $\Phi_D + \Phi_R$ (dispersion plus repulsion) terms are known as the London or van der Waals forces. Spherical, nonpolar molecules are well described by the familiar Lennard-Jones 6–12 potential equation:

$$\Phi_D + \Phi_R = 4\varepsilon\left[-(\sigma/r)^6 + (\sigma/r)^{12}\right]$$

where r is the intermolecular separation distance, and σ (length units) and ε (energy units) are constants characteristic of the colliding molecules. Values of force constants σ and ε have been compiled (2).

These forces arise from the fact that each molecule contains atoms having a nucleus and surrounded by a cloud of electrons. The electron cloud fluctuates and is nonsymmetrical at various instants in time. Although a nonpolar neutral molecule has no net permanent charge or dipole, these fluctuating electron distributions provide fluctuating dipoles in each molecule. These fluctuating dipoles interact to generate forces between molecules or between adsorbed molecules and adsorbent surfaces. These contributions to the potential energy of adsorption are present even if the adsorbed molecules are nonpolar and even if the adsorbent structure contains no strong electrostatic fields.

The contribution Φ_P is due to the polarization of the molecules by electric fields on the adsorbent surface, eg, electric fields between positively charged cations and the negatively charged framework of a zeolite adsorbent. The attractive interaction between the induced dipole and the electric field is called the polarization contribution. Its magnitude is dependent on the polarizability α of the molecule and the strength of the electric field F of the adsorbent (4): $\Phi_P = -1/2\alpha F^2$.

The first of the two specific interaction terms $\Phi_{F-\mu}$ is due to the attractive interaction between the permanent dipole moment μ of a molecule and the electric field on the adsorbent surface (4):

$$\Phi_{F-\mu} = -F\mu\cos\Theta$$

where Θ is the dipole–axis/field angle.

The other specific interaction term $\Phi_{\delta F-Q}$ is due to the attractive interaction between the permanent quadrupole moment Q of the molecule and the electric

field gradient on the adsorbent surface (4):

$$\Phi_{\delta F-Q} = \frac{1}{2} Q\, dF/dR$$

The final contribution, the self-potential term Φ_{SP}, is the sum of all the above interactions of adsorbed molecules with each other.

Finally, an analysis of the energies of adsorption on many practical polar and nonpolar adsorbents has shown not only that the magnitude of the Φ_P term depends directly on the polarizability α, but also that the sum of all of the nonspecific terms taken together, ie, $\Phi_D + \Phi_R + \Phi_P$, increases monotonically, with increasing α (4).

2.2. Adsorption Selectivities. For a given adsorbent, the relative strength of adsorption of different adsorbate molecules depends on the relative magnitudes of the polarizability α, dipole moment μ, and quadrupole moment Q of each. These properties for some common molecules are given in Table 2. Often, just the consideration of the values of α, μ, and Q allows accurate qualitative predictions to be made of the relative strengths of adsorption of given molecules on an adsorbent or of the best adsorbent type (polar or nonpolar) for a particular separation.

For example, the strength of the electric field F and field gradient ($\delta F = dF/dr$) of the highly polar cationic zeolites is strong. For this reason, nitrogen is more strongly adsorbed than is oxygen on such adsorbents, primarily because of the stronger quadrupole of N_2 compared to O_2.

In contrast, nonpolar activated carbon adsorbents lack strong electric fields and field gradients. Such adsorbents adsorb O_2 slightly more strongly than N_2, because of the slightly higher polarizability of O_2. Relative selectivities on nonpolar adsorbents often parallel the relative volatilities of the same compounds. Compounds with higher boiling points are more strongly adsorbed. In this

Table 2. **Electrostatic Properties of Some Common Molecules**

Molecule	Polarizability $\alpha \times 10^{40}$, $C^2 \cdot m^2/J$ [a]	Dipole moment $\mu \times 10^{30}$, C·m [b]	Quadrupole moment $Q \times 10^{40}$, $C \cdot m^2$ [c]
Ar	1.83	0.00	0.00
H_2	0.90	0.00	2.09
N_2	0.78	0.00	−4.91
O_2	1.77	0.00	−1.33
CO	2.19	0.37	−6.92
CO_2	3.02	0.00	−13.71
CS_2	9.41	0.00	12.73
N_2O	3.32	0.54	−12.02
NH_3	2.67	5.10	−7.39
C_2H_6	4.97	0.00	−3.32
C_6H_6	11.49	0.00	−30.7
HCl	2.94	3.57	13.28

[a] To convert $C^2 \cdot m^2/J$ to cm^3, divide by 1.113×10^{-16}.

[b] To convert C·m to debyes, divide by 3.336×10^{-30}.

[c] To convert $C \cdot m^2$ to Buckinghams, divide by 3.336×10^{-40}.

case, the higher boiling O_2 (bp $\sim$ 90 K) is more strongly adsorbed than is N_2 (bp $\sim$ 77 K).

The polarizabilities of molecules in a homologous series increase steadily with increasing numbers of atoms. Therefore, the relative strengths of adsorption also increase (along with the boiling points).

For a given adsorbate molecule, the relative strength of adsorption on different adsorbents depends largely on the relative polarizability and electric field strengths of adsorbent surfaces. On the one hand, water molecules, with relatively low polarizability but a strong dipole and moderately strong quadrupole moment, are strongly adsorbed by polar adsorbents (eg, cationic zeolites), but only weakly adsorbed by nonpolar adsorbents (eg, silicalite or nonoxidized forms of activated carbon). On the other hand, saturated hydrocarbons with low molecular weight have greater polarizabilities than does water, but no dipoles and only weak quadrupoles. These molecules are adsorbed less strongly than water on polar adsorbents, but more strongly than water on nonpolar adsorbents. Therefore, polar adsorbents are often called hydrophilic adsorbents and nonpolar adsorbents are called hydrophobic adsorbents.

2.3. Isotherms and Isobars. The graphical presentation of the equilibrium adsorbate loading vs adsorbate pressure (or concentration) at constant temperature (Fig. 1) is an adsorption isotherm. A graph of the adsorbate loading vs temperature at constant adsorbate pressure (Fig. 2) is an adsorption isobar. The greater the strength of adsorption, the greater is the adsorbate loading at a given temperature and partial pressure of the adsorbate up to the point where the maximum adsorption capacity of the adsorbent has been attained.

The strength of adsorption of unsaturated hydrocarbons by a polar adsorbent (zeolite) is much greater than for saturated hydrocarbons, and increases with increasing carbon number (Fig. 3). This observation may be understood as a consequence of the increasing polarizability of molecules with increasing

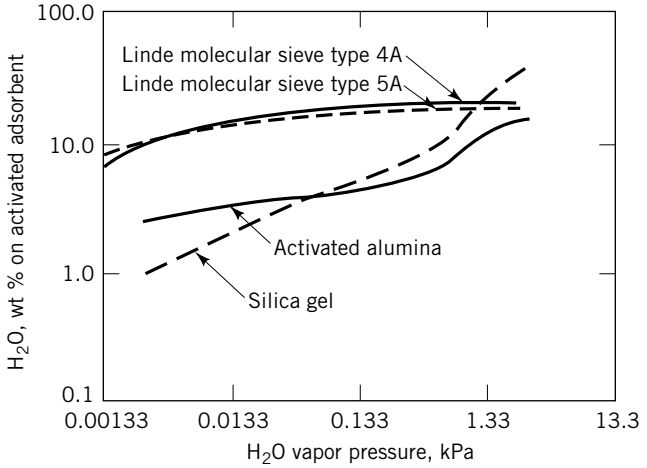

Fig. 1. Water isotherms for various adsorbents (1). Activation conditions: Linde molecular sieves, 350°C and <1.33 Pa; activated alumina, 350°C and <1.33 Pa; silica gel, 175°C and <1.33 Pa. To convert kPa to mm Hg, divide by 0.133.

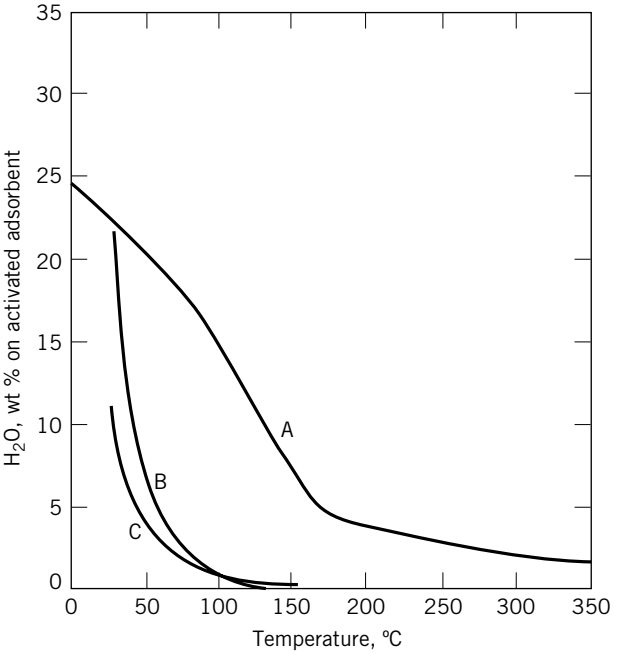

Fig. 2. Water isobars for various adsorbents: Equilibrium H_2O capacity vs temperature for three adsorbents (1); $p_{H_2O} = 1.33$ kPa (10 mm Hg) at 12°C and 101.3 kPa (1 atm). Activation conditions: A, Linde molecular sieve, 350°C and <1.33 Pa; B, activated alumina, 350°C and <1.33 Pa; C, silica gel, 175°C and <1.33 Pa. To convert Pa to mm Hg, multiply by 0.0075.

numbers of bonds and the presence of dipole and stronger quadrupole moments in the unsaturated hydrocarbons compared to the saturated hydrocarbons.

2.4. Heats of Adsorption. Physical adsorption processes are exothermic, ie, they release heat. Because the entropy change ΔS on adsorption is negative (adsorbed molecules are more ordered than in the gas phase) and the free energy change ΔG must be negative for adsorption to be favored, thermodynamics ($\Delta G = \Delta H - T\Delta S$) requires the enthalpy change ΔH on adsorption (heat of adsorption) to be negative (exothermic). Adsorption strengths thus decrease with increasing temperature.

The integral heat of adsorption is the total heat released when the adsorbate loading is increased from zero to some final value at isothermal conditions. The differential heat of adsorption δH_{iso} is the incremental change in heat of adsorption with a differential change in adsorbate loading. This heat of adsorption δH_{iso} may be determined from the slopes of adsorption isosteres (lines of constant adsorbate loading) on graphs of ln P vs $1/T$ (Fig. 4) through the Clausius-Clapeyron relationship:

$$\frac{d \ln P}{d\,(1/T)} = -\frac{\delta H_{iso}}{R}$$

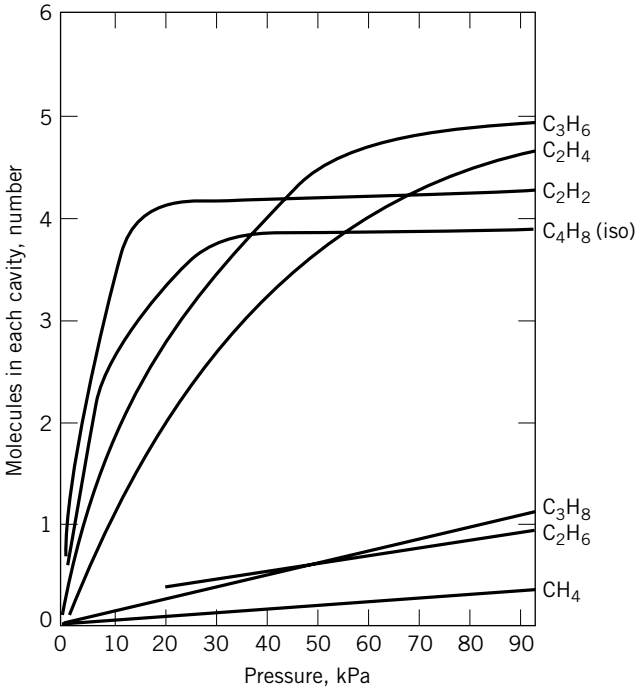

Fig. 3. Adsorption of hydrocarbons by zeolites is much greater for unsaturated hydrocarbons whose molecules contain double or triple bonds. From top to bottom, the curves show adsorption (at 150°C) of propylene, ethylene, acetylene, and isobutylene (unsaturated) and propane, ethane, and methane (saturated) (5). To convert kPa to mm Hg, multiply by 7.5. Courtesy of *Scientific American*.

where R is the gas constant, P the adsorbate absolute pressure, and T the absolute temperature.

Differential heats of adsorption for several gases on a sample of a polar adsorbent (natural zeolite chabazite) are shown as a function of the quantities adsorbed in Figure 5. Consideration of the electrical properties of the adsorbates, included in Table 2, allows the correct prediction of the relative order of adsorption selectivity:

$$\mathrm{Ar} < \mathrm{O_2} < \mathrm{N_2} < \mathrm{CO} \ll \mathrm{CO_2}$$

At low adsorbate loadings, the differential heat of adsorption decreases with increasing adsorbate loadings. This is direct evidence that the adsorbent surface is energetically heterogeneous, ie, some adsorption sites interact more strongly with the adsorbate molecules. These sites are filled first so that adsorption of additional molecules involves progressively lower heats of adsorption.

All practical adsorbents have surfaces that are heterogeneous, both energetically and geometrically (not all pores are of uniform and constant dimensions). The degree of heterogeneity differs substantially from one adsorbent type to another. These heterogeneities are responsible for many nonlinearities, both in single component isotherms and in multicomponent adsorption selectivities.

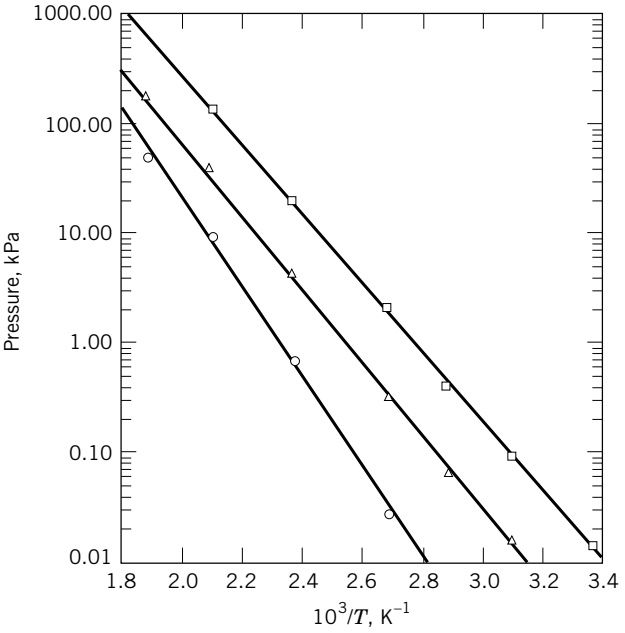

Fig. 4. Adsorption isosteres, water vapor on 4A (NaA) zeolite pellets (6). H_2O loading: □, 15 kg/100 kg zeolite; △, 10 kg/100 kg, ○, 5 kg/100 kg. To convert kPa to mm Hg, multiply by 7.5. Courtesy of Union Carbide.

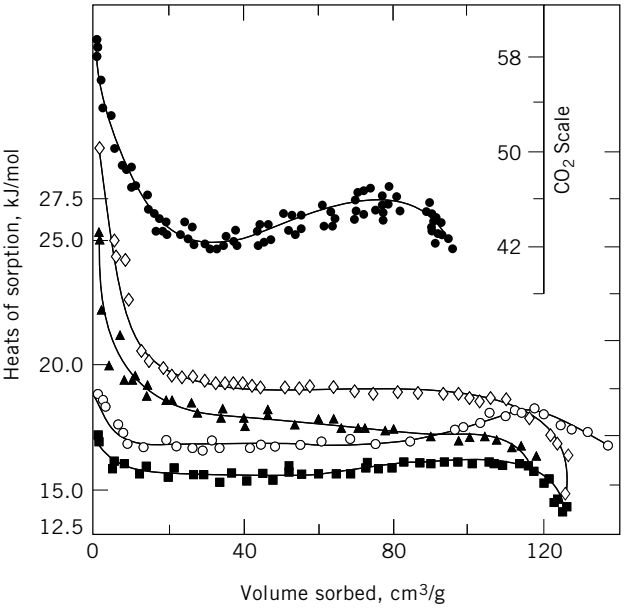

Fig. 5. Differential heats of sorption in nature chabazite (4). ▲ = N_2; ■ = Ar; ○ = O_2; ◇ = CO; ● = CO_2. See Table 2 for polarizability, dipole moment, and quadrupole moment values for the gases. Volume adsorbed is expressed as cm^3 of adsorbate as liquid. To convert kJ to kcal, divide by 4.184. Courtesy of Academic Press.

In Figure 5, the heat of adsorption of CO_2 increases slightly at the higher adsorbate loadings. This increase is due to the increasing self-potential contribution at the higher loadings.

2.5. Isotherm Models. Many efforts have been made over the years to develop isotherm models for data correlation and design predictions for both single component and multicomponent adsorption. Unfortunately, no single model is accurate over broad ranges of adsorbent and adsorbate types, pressures, temperatures, and loadings, especially for multicomponent systems. The reason is probably due to deficiencies in the models in adequately describing both the heterogeneities of the surface and the effects of the adsorbate on the properties of the adsorbent itself. Most models assume the adsorbent is inert, ie, not altered by the presence of the adsorbate molecules; however, partial changes in some adsorbent properties are commonly observed.

Nevertheless, each of the more popular isotherm models have been found useful for modeling adsorption behavior in particular circumstances. The following outlines many of the isotherm models presently available. Detailed discussions of derivations, assumptions, strengths, and weaknesses of these and other isotherm models are given in (4,7–16).

Not all of the isotherm models discussed next are rigorous in the sense of being thermodynamically consistent. For example, specific deficiencies in the Freundlich, Sips, Dubinin-Radushkevich, Toth, and vacancy solution models have been identified (14).

The Sips and related loading ratio correlation (LRC) models fail to properly predict Henry's law behavior (as required for thermodynamic consistency) at the zero pressure limit (8). Thermodynamic inconsistency of the LRC model had also been noted by the original authors (17); nevertheless, the model has been found useful in predicting multicomponent performance from single component data and correlating multicomponent data (18). However, users of models lacking thermodynamic consistency must take due care, particularly in extrapolation beyond the range of actual experimental data.

Because the Dubinin, Langmuir, and modified Langmuir (or LRC) do a very good job of fitting data over broad ranges of parameters, several authors had made modifications to them to make them thermodynmically consistent. The Dubinin equations have been modified to have a proper Henry's law region (19). A consisent dual site Langmuir model has been offered (20). The LRC equations have been extended to have correct Henry's law behavior and to be thermodynamically consistent (21).

Thermodynamically Consistent Isotherm Models. These models include both the statistical thermodynamic models and the models that can be derived from an assumed equation of state for the adsorbed phase plus the thermodynamics of the adsorbed phase, ie, the Gibbs adsorption isotherm,

$$\left(\frac{d\Phi}{dP}\right)_T = \frac{qRT}{P}$$

where Φ is the spreading pressure, P the partial pressure of adsorbate, q the adsorbate loading x per quantity w of adsorbent $= x/w$, T the temperature, and R the gas constant. In the following models, $\Theta = q/q_{\max}$ is the fractional

surface coverage, where q_{max} is the maximum loading. Constants are q_{max}, all K's, all k's, all A's, *b, c, n, s, t*, β, and τ. The vapor pressure of pure adsorbate is P_0.

$$\begin{aligned}
\text{Henry's law}: &\quad q = KP_0 \\
\text{Langmuir}: &\quad K'P_0 = \Theta/(1-\Theta) \\
\text{Volmer}: &\quad bP_0 = [\Theta/(1-\Theta)]\exp[\Theta/(1-\Theta)] \\
\text{van der Waals}: &\quad K''P_0 = [\Theta/(1-\Theta)]\exp[\Theta/(1-\Theta)]\exp[B/RT] \\
\text{Virial}: &\quad K'''P_0/x = \exp\left[2A_1x + \left(\tfrac{3}{2}\right)A_2x^2 + \cdots\right]
\end{aligned}$$

The Langmuir model is discussed in (22); the Volmer in (23); and the van der Waals and virial equations in (8).

Statistical Thermodynamic Isotherm Models. These approaches were pioneered by Fowler and Guggenheim (24) and Hill (25). Examples of the application of this approach to modeling of adsorption in microporous adsorbents are given in (3,26–30). Excellent reviews have been written (4,31).

Semiempirical Isotherm Models. Some of these models have been shown to have some thermodynamic inconsistencies and should be used with due care. Nevertheless, they have each been found to be useful for data correlation and interpolation, as well as for the calculation of some thermodynamic properties.

Polanyi Adsorption Potential. These models are based on the adsorption potential

$$A = RT\ln(P_0/P)$$

The Dubinin-Radushkevich model (32) is the same as the more general Dubinin-Astakhov equation (33) (see below), with $n = 2$.

The Dubinin-Astakhov model is

$$\Theta = \exp[-(A/E)^n]$$

where n is generally between 1 and 3.

Radke-Prausnitz. This model (34) is also known as the Langmuir-Freundlich model:

$$\Theta = \frac{k'P}{[1+(k'P)]^{\tau}}$$

Toth. This model (35) is represented as

$$\Theta = \frac{kP}{[1+(kP^t)^{1/t}]}$$

UNILAN. The uniform distribution, Langmuir local isotherm model (12):

$$\Theta = \frac{1}{2s}\ln\left[\frac{(c+Pe^s)}{(c+Pe^{-s})}\right]$$

BET. This model (36) estimates the coverage corresponding to one monolayer of adsorbate and is used to measure the surface areas of solids:

$$\Theta = \frac{b(P/P_0)}{[(1 - P/P_0)\,(1 - P/P_0 + bP/P_0)]}$$

Isotherm Models for Adsorption of Mixtures. Of the following models, all but the ideal adsorbed solution theory (IAST) and the related heterogeneous ideal adsorbed solution theory (HIAST) have been shown to contain some thermodynamic inconsistencies. References to the limited available literature data on the adsorption of gas mixtures on activated carbons and zeolites have been compiled, along with a brief summary of approximate percentage differences between data and theory for the various theoretical models (16). In the following models the subscripts i and j refer to different adsorbates.

Markham and Benton. This model (37) is known as the extended Langmuir isotherm equation for two components, i and j:

$$\Theta_i = K_i P_i / \left(1 + K_i P_i + K_j P_j\right)$$
$$\Theta_j = K_j P_j / \left(1 + K_i P_i + K_j P_j\right)$$

Leavitt Loading Ratio Correlation (LRC) Method. The LRC model (17) for a single component i parallels Sips model (38):

$$\Theta_i = (K_i P_i)^{1/n_i} \Big/ \left[1 + (K_i P_i)^{1/n_i}\right]$$

but with

$$-\ln K_i = A_{1i} + A_{2i}/T$$

For the binary system of components i and j, the LRC model (17) is

$$\Theta_i = (K_i P_i)^{1/n_i} \Big/ \left[1 + (K_i P_i)^{1/n_i} + \left(K_j P_j\right)^{1/n_j}\right]$$

Ideal Adsorbed Solution (IAS) Model. For components i and j, assuming ideal gas behavior, this model (39) is

$$\frac{\Phi A}{RT} = \int_0^{P_i^o} \left[q_i^o(P)\right] d(\ln P) = \int_0^{P_j^0} \left[q_j^0(P)\right] d(\ln P)$$

$$PY_i = P_i^0 X_i$$

$$PY_j = P_j^0 X_j = P_j^0 (1 - X_i)$$

where P_i° is the vapor pressure of component i, $q_i^{\circ}(P)$ the equilibrium loading of pure i at pressure P, Y_i the vapor-phase mole fraction of component i, and X_i the adsorbed phase mole fraction of component i. These equations are solved

simultaneously to determine P_i^o, P_j^o, and X_i, and the following equations are used to calculate q_i, q_j, and q_{total}:

$$1/q_{\text{total}} = X_i/\lfloor q_i(P_i^0)\rfloor + X_j/\lfloor q_j(P_j^0)\rfloor$$

$$q_i = q_{\text{total}}X_i$$

$$q_j = q_{\text{total}}X_j$$

Heterogeneous Ideal Adsorbed Solution Theory (HIAST). This IAS theory has been extended to the case of adsorbent surface energetic heterogeneity and is shown to provide improved predictions over IAST (12).

Vacancy Solution Model (VSM). The initial model (40) considered the adsorbed phase to be a mixture of adsorbed molecules and vacancies (a vacancy solution) and assumed that nonidealities of the solution can be described by the two-parameter Wilson activity coefficient equation. Subsequently, it was found that the use of the three-parameter Flory-Huggins activity coefficient equation provided improved prediction of binary isotherms (41).

2.6. Molecular Modeling. Since the 1980s, significant advances have been made in molecular modeling of adsorption (42,43). The availability of high speed computers has made it practical to model adsorbate–adsorbent interactions in micro- and meso-pores using statistical thermodynamic principles. Many universities and research organizations have developed Monte Carlo computer programs; a commercial simulation program, Cerius2, is available from Molecular Simulation Inc. Adsorbent pores have been modeled in various ways to predict adsorption equilibrium and diffusivity phenomenon—as flat surfaces, as narrow slits, and as the regular crystalline structures of zeolites. The results vary greatly depending on such choices. Monte Carlo simulation has been used as an aid in the design of zeolites (44) and of activated carbons (45). Molecular modeling has been used to study pore size distribution by varying slit width (45) and to interpret NMR data (46).

2.7. Adsorption Dynamics. An outline of approaches that have been taken to model mass-transfer rates in adsorbents has been given (see ADSORPTION). Detailed reviews of the extensive literature on the interrelated topics of modeling of mass-transfer rate processes in fixed-bed adsorbers, bed concentration profiles, and breakthrough curves include (16,29). The related simple design concepts of WES, WUB, and LUB for constant-pattern adsorption are discussed later.

2.8. Reactions on Adsorbents. To permit the recovery of pure products and to extend the adsorbent's useful life, adsorbents should generally be inert and not react with or catalyze reactions of adsorbate molecules. These considerations often affect adsorbent selection and/or require limits be placed upon the severity of operating conditions to minimize reactions of the adsorbate molecules or damage to the adsorbents. However, even then, gradual reactions of trace impurities in a feed stream or slowly occurring reactions that modify the adsorbent may still cause a gradual decline in the adsorbent performance, as illustrated in Figure 6.

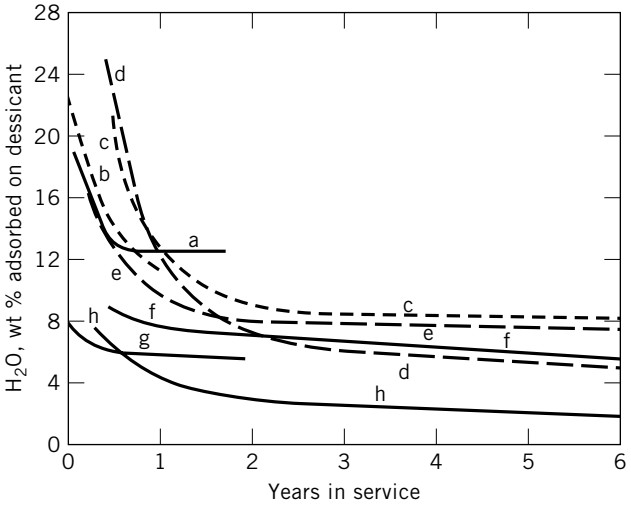

Fig. 6. Adsorption capacity of various dessicants vs years of service in dehydrating high pressure natural gas (47). (**a**) Alumina H-151, gas ~27°C and 123 kPa, from oil and water separators; (**b**) silica gel, gas ~38°C and 145 kPa, from oil absorption plant; (**c**) sorbead, 136-kPa gas from absorption plant; regeneration gas inlet temperature 243°C (maximum allowable dew point −6.7°C); (**d**) sorbead, 40-kPa gas containing propane; regeneration gas temperature 177°C (maximum allowable dew point −34°C); (**e**) sorbead, 1950–1956 data; (**f**) activated alumina, same gas as for Curve **d**; (**g**) activated bauxite(florite), residue gas from gasoline absorption plant; (**h**) activated alumina, same gas for for Curve **c**. Courtesy of Gulf Publishing Company.

3. Adsorbent Principles

3.1. Principal Adsorbent Types. Commercially useful adsorbents can be classified by the nature of their structure (amorphous or crystalline), by the sizes of their pores (micropores, mesopores, and macropores), by the nature of their surfaces (polar, nonpolar, or intermediate), or by their chemical composition. All of these characteristics are important in the selection of the best adsorbent for any particular application.

However, the size of the pores is the most important initial consideration because, if a molecule is to be adsorbed, it must not be larger than the pores of the adsorbent. Conversely, by selecting an adsorbent with a particular pore diameter, molecules larger than the pores may be selectively excluded, and smaller molecules can be allowed to adsorb.

Pore size is also related to surface area and thus to adsorbent capacity, particularly for gas-phase adsorption. Because the total surface area of a given mass of adsorbent increases with decreasing pore size, only materials containing micropores and small mesopores (nanometer diameters) have sufficient capacity to be useful as practical adsorbents for gas-phase applications. Micropore diameters are <2 nm; mesopore diameters are between 2 and 50 nm; and macropores diameters are >50 nm, by International Union of Pure and Applied Chemistry (IUPAC) classification (48).

The practical adsorbents used in most gas-phase applications are limited to the following types, classified by their amorphous or crystalline nature.

- *Amorphous*: silica gel, activated alumina, activated carbon, molecular sieve carbons and macroreticular resins.
- *Crystalline*: molecular sieve zeolites, and related molecular sieve materials that are not technically zeolites, eg, silicalite, $AlPO_4$s, and SAPOs, as well as mesoporous silicates/aluminosilicates, eg, MCM-41.

Typical pore size distributions for these adsorbents have been given (see ADSORPTION). Only molecular sieve carbons and crystalline molecular sieves have large pore volumes in pores <1 nm. Only the crystalline molecular sieves have monodisperse pore diameters because of the regularity of their crystalline structures (49).

Activated carbons are made by first preparing a carbonaceous char with low surface area followed by controlled oxidation in air, carbon dioxide, or steam. The

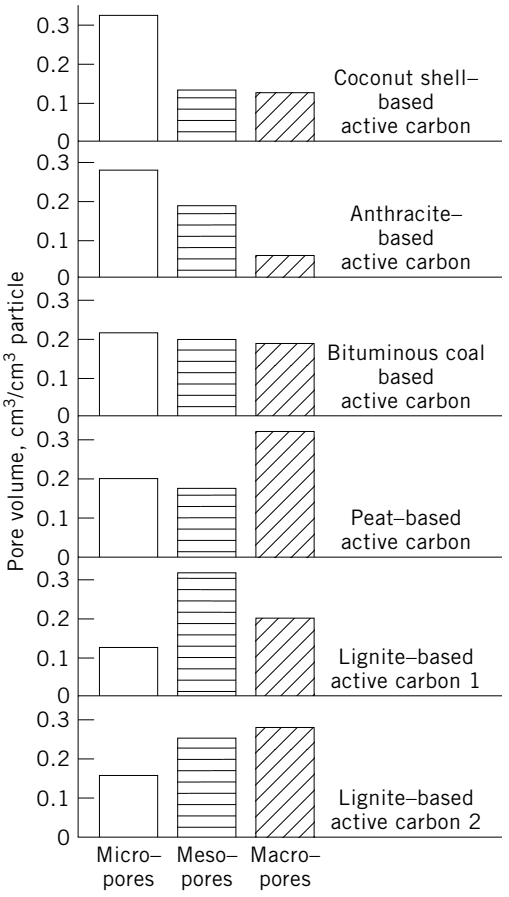

Fig. 7. Pore size distribution in some active carbons obtained using different precursors (50).Courtesy of Marcel Dekker Publishing Company.

pore-size distributions of the resulting products are highly dependent on both the raw materials and the conditions used in their manufacture, as may be seen in Figure 7.

Assuming the pores are large enough to admit the molecules of interest, the most important consideration is the nature of the adsorbent surface, because this characteristic controls adsorption selectivity.

Practical adsorbents may also be classified according to the nature of their surfaces.

- *Highly polar*: molecular sieve zeolites with high aluminum and cation contents.
- *Moderately polar*: crystalline molecular sieves with low aluminum and low cation contents, silica gel, activated alumina, activated carbons with highly oxidized surfaces, crystalline molecular sieve $AlPO_4$'s.
- *Nonpolar*: silicalite, F-silicalite, other high silica content crystalline molecular sieves, activated carbons with reduced surfaces.

3.2. Adsorption Properties. Typical adsorption isotherms for water on various adsorbents are given in Figure 1, and the corresponding isobars in Figure 2. Not only do the more highly polar molecular sieve zeolites adsorb more water at lower pressures than do the moderately polar silica gel and alumina gel, but they also hold onto the water more strongly at higher temperatures. For the same reason, temperatures required for thermal regeneration of water-loaded zeolites is higher than for less highly polar adsorbents.

Isotherms for H_2O and *n*-hexane adsorption at room temperature and for O_2 adsorption at liquid oxygen temperature on 13X (NaX) zeolite and on the crystalline SiO_2 molecular sieve silicalite are are shown in Figure 8. Silicalite adsorbs water very weakly. Further modification of silicalite by fluoride incorporation provides an extremely hydrophobic adsorbent, shown in Figure 9. These examples illustrate the broad range of properties of crystalline molecular sieves.

Activated carbons contain chemisorbed oxygen in varying amounts unless special care is taken to eliminate it. Desired adsorption properties often depend on the amount and type of chemisorbed oxygen species on the surface. Therefore, the adsorption properties of an activated carbon adsorbent depend on its prior temperature and oxygen-exposure history. In contrast, molecular sieve zeolites and other oxide adsorbents are not affected by oxidizing or reducing conditions.

This principle is illustrated in Figure 10. Water adsorption at low pressures is markedly reduced on a poly(vinylidene chloride)-based activated carbon after removal of surface oxygenated groups by degassing at 1000°C. Following this treatment, water adsorption is dominated by capillary condensation in mesopores, and the size of the adsorption–desorption hysteresis loop increases, because the pore volume previously occupied by water at the lower pressures now remains empty until the water pressure reaches pressures ($\sim$0.3 to 0.4 times the vapor pressure) at which capillary condensation can occur.

Typical adsorption isotherms for light hydrocarbons on activated carbon prepared from coconut shells are shown in Figure 11. The polarizabilities and

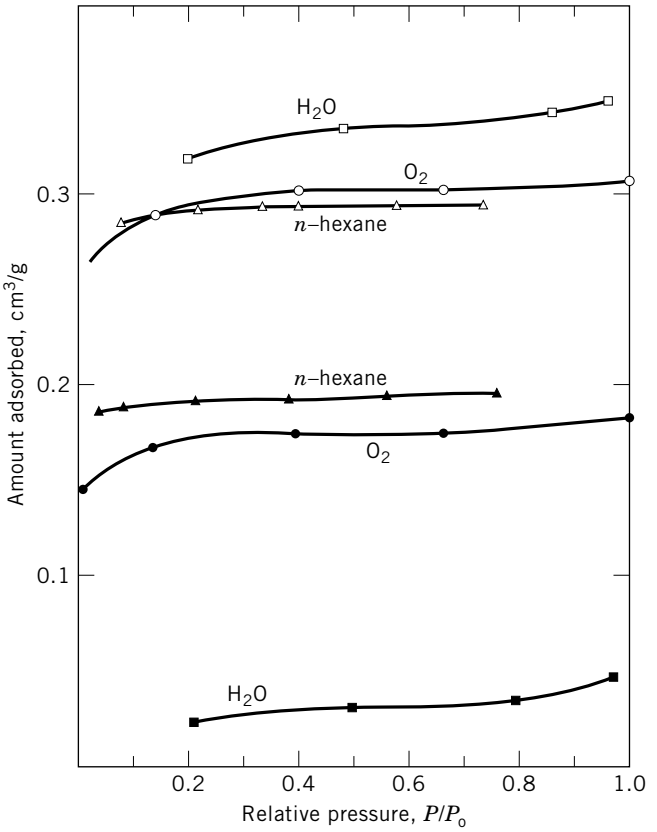

Fig. 8. Adsorption isotherms of H_2O, O_2, and n-hexane on zeolite NaX (open symbols) and silicalite (filled symbols). Oxygen is at $-183°C$ and water and n-hexane (C_6H_{14}) at room temperature (RT). Volume adsorbed is expressed as cm^3 of adsorbate as liquid. Courtesy of *Nature, London* (51).

boiling points of these compounds increase in the order

$$CH_4 < C_2H_4 < C_2H_6 < C_3H_6 < C_3H_8$$

The relative strengths of adsorption of these compounds follow the same order, as expected for a nonpolar adsorbent, except that C_3H_6 was adsorbed more strongly than C_3H_8. This result indicates that the surface is weakly polar and that specific (dipole–field and quadrupole–field gradient) contributions to the adsorption potential alter the expected order slightly. This situation may also be due to chemisorbed oxygen species on the surface.

3.3. Physical Properties. Physical properties of importance include particle size, density, volume fraction of intraparticle and extraparticle voids when packed into adsorbent beds, strength, attrition resistance, and dustiness. Any of these properties can be varied intentionally to tailor adsorbents to specific applications (See ADSORPTION LIQUID SEPARATION; CARBON, ACTIVATED CARBON; ION EXCHANGE; MOLECULAR SIEVES; AND SILICON COMPOUNDS, SYNTHETIC INORGANIC SILICATES).

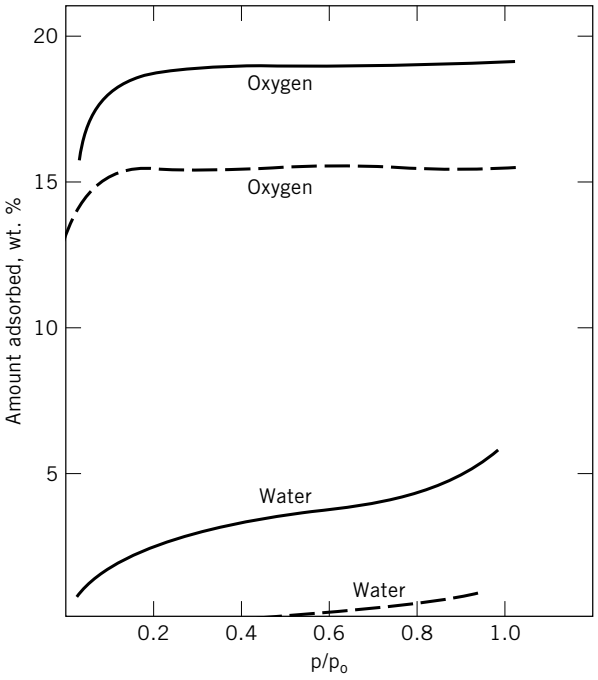

Fig. 9. Adsorption of oxygen (90 K) and water (RT) on silicalite (—) and F-silicalite (– – –) (52).

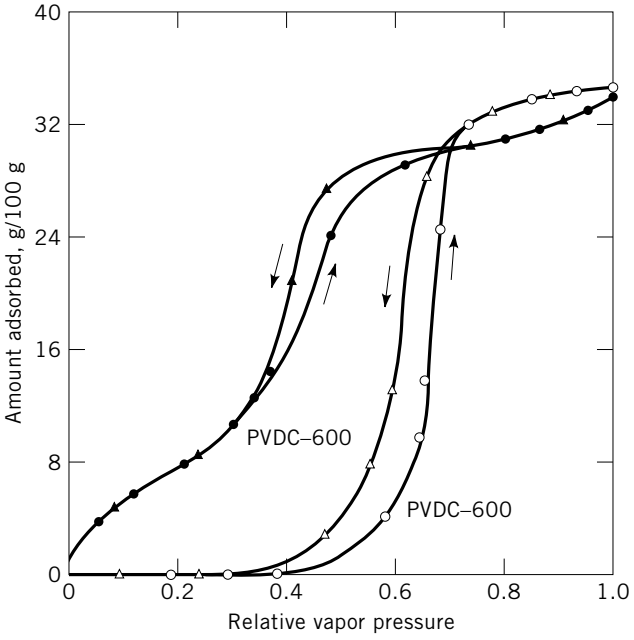

Fig. 10. Adsorption (●, ○)-desorption (▲, △) isotherms of water vapor on poly(vinylidene chloride) (PVDC) carbon before (filled symbols) and after (open symbols) outgassing at 1000°C (53). Courtesy of *Carbon*.

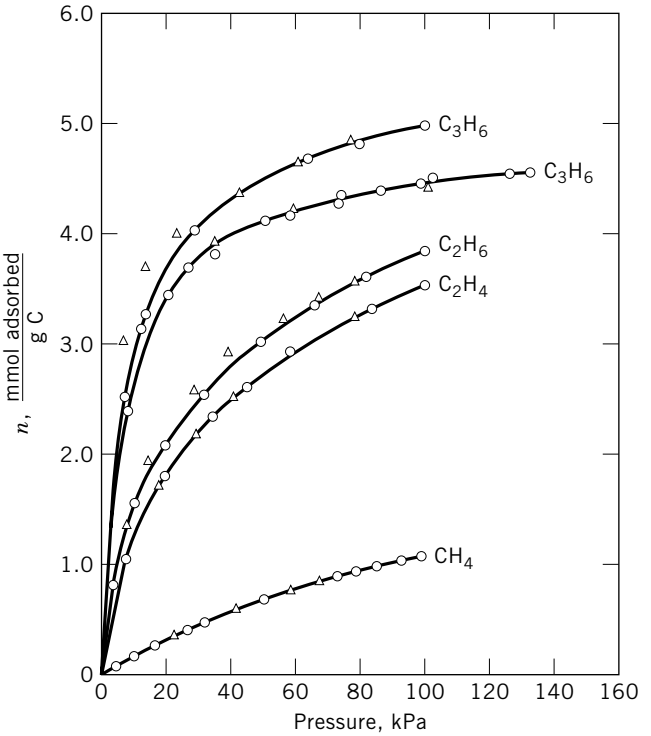

Fig. 11. Adsorption isotherms for hydrocarbons on activated coconut-shell carbon at 25°C (54). ○, Adsorption; △, desorption. To convert kPa to mm Hg, multiply by 7.5. Courtesy of *Industrial and Engineering Chemistry*.

Most commercial adsorbents for gas-phase separations are employed in the form of pellets, beads, or granular shapes, typically ∼1.5–3.2 mm in size. However, a growing number of atmospheric presssure applications are employing adsorbents in the form of honeycomb monoliths and fabrics. These configurations have been introduced to reduce the pressure drop and thus utility consumption.

3.4. Deactivation. All adsorbents, no matter how inert, will be deactivated during extended usage by reaction with inpurities, reaction of adsorbates, or thermal damage. To compensate, adsorbent beds are sized to account for the gradual loss in capacity and to allow their use for a given period of time. Most commonly, at the end of its useful life, the adsorbent is dumped from the beds and replaced with fresh adsorbent.

The most common degradation when hydrocarbons are present is the formation of "coke" (high molecular weight, high carbon to hydrogen ratio material). Depending on conditions, coke formed from unsaturated hydrocarbons can be found on adorption sites reducing capacity, in pores decreasing mass transfer, or on the external surface (55). In some cases, the process equipment can be designed to allow periodic *in situ* rejuvenation of the adsorbent, eg, a periodic burning-off of coke accumulated on the adsorbent.

Adsorbent degradation by chemical attack or physical damage is not reversible. Acids or acid gases can react with adsorbents with alkaline surface

chemistry, eg, low silica zeolites, and cause loss of adsorption capacity. Other adsorbents, such as silica gel high silica zeolites, are sensitive to alkalies. Oxidative or reductive conditions can change the adsorptive surface characteristics of activated carbon. The constant thermal expansion and contraction in temperature-swing adsorption (TSA) processes can cause damage to the internal pore and/or crystal structure. Activated alumina and silica gel can be dehydrated by excessive temperatures. When water is present, hydrothermal cycling can cause explosive steam release that physically damages some adsorbents. Some types of silica gel are susceptible to breakup caused by water droplets; special decrepitation-resistant grades are available.

4. Adsorption Processes

Adsorption processes are often identified by their method of regeneration. Pressure-swing adsorption (PSA) and TSA are the most frequently applied process cycles for gas separation. Purge-swing cycles and nonregenerative approaches are also applied to the separation of gases. Special applications exist in the nuclear industry. Others take advantage of reactive sorption. Most adsorption processes use fixed beds, but some use moving or fluidized beds, or rotary wheels.

4.1. Temperature Swing. A temperature-swing or TSA cycle is one in which desorption takes place at a temperature much higher than adsorption. The principal application is for separations in which contaminants are present at low concentration, ie, for purification. The TSA cycles are characterized by low residual loadings and high operating loadings. Figure 12 depicts the isotherms for the two temperatures of a TSA cycle. The available operating capacity is the difference between the loadings X_1 and X_2. These high adsorption capacities for low concentrations mean that cycle times are long, hours to days, for reasonably sized beds. This long cycle time is fortunate, because packed beds of adsorbent respond slowly to changes in gas temperature. A purge and/or vacuum removes the thermally desorbed components from the bed, and cooling returns the bed to adsorption condition. Systems in which species are strongly adsorbed are especially suited to TSA. Such applications include drying, sweetening, CO_2 removal, and pollution control.

Principles. In a TSA cycle, two processes occur during regeneration: heating and purging. Heating must provide adequate thermal energy to raise the adsorbate, adsorbent and adsorber temperature, desorb the adsorbate, and make up for heat losses. Regeneration is heating limited (or stoichiometric limited) when transfer of energy to the system is limiting. Equilibrium determines the maximum capacity of the purge gas to transfer the desorbed material away. Regeneration is stripping limited (or equilibrium limited) when transferring adsorbate away is limiting.

Heating occurs by either direct (external heat exchange to the purge gas) or, less commonly, indirect (heating elements, coils or panels, inside the adsorber) contact of the adsorbent by the heating medium. Direct heating is simpler and is invariably used for stripping-limited regeneration. Alternate methods for supplying indirect heat for desorption are microwave fields and joule's heat (electrothermal). Microwave energy has been successfully applied to regeneration of

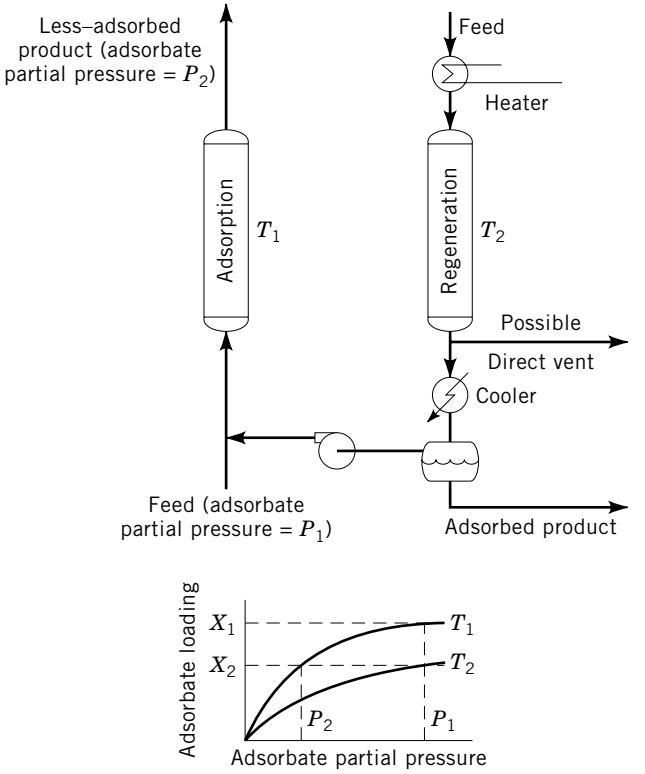

Fig. 12. Temperature-swing cycle (1). Loading X_1 at T_1 and feed partial pressure P_1; X_2 at the higher T_2 and the lower P_2 needed in the product.

low and high silica zeolites, activated carbon, and macroreticular resins (56). The electrical conductivity of carbon has been utilized to generate indirect heat in activated carbon adsorbers made of cloth (57) of granules (58), and of beads (59). However, the complexity of all of these indirect heating methods limits their use to heating-limited regeneration where purge gas is in short supply. Coils or panels can supply indirect cooling as well. The use of steam for the regeneration of activated carbon is a combination of thermal desorption and purge displacement; direct heating is supplied by water adsorption.

Steps. Thermal-swing cycles have at least two steps: adsorption and heating. A cooling step is also normally used after the heating step. A portion of the feed or product stream can be utilized for heating, or an independent fluid can be used. Easily condensable contaminants may be regenerated with noncondensable gases and recovered by condensation. Water-immiscible solvents are stripped with steam, which may be condensed and separated from the solvent by decantation. Fuel and/or air may be used when the impurities are to be burned or incinerated.

The highest regeneration temperatures are the most efficient for desorption. However, heater cost, metallurgy, and the thermal stability of the adsorbent and the fluids must be considered. Silica gel requires the lowest temperatures and the lowest amount of heat of any commercial adsorbent. Activated

carbons, aluminas, and high silica molecular sieves can tolerate the highest temperatures. Although thermal-swing regeneration can be done at the same pressure as adsorption, lowering the pressure can achieve better desorption and is often used; such cycles are actually a hybrid of PSA and TSA referred to as pressure/thermal swing adsorption (PTSA). The heating gas is normally used for the cooling step. Rather than cooling the bed, adsorption can sometimes be started on a hot bed. If certain criteria are met (60), the dynamic adsorption performance does not depend on cooling.

Flow Sheet. The most common processing scheme is a pair of fixed-bed adsorbers alternating between the adsorption step and the regeneration steps. An example is given in Figure 12. However, the variations possible to achieve special needs are endless. The flow directions can be varied. Single beds provide interrupted flow, but multiple beds can ensure constant flow. Beds can be configured in lead-trim, parallel trains, series cool-heat, or closed-loop. Regeneration may even be *ex situ* rather than *in situ*.

The normal flow direction through a fixed bed is usually in a vertical direction. The mechanical complexities required for horizontal- or annular-flow beds often outweigh the decrease in pressure drop achieved. Because allowable velocities for crushing exceed those for lifting, the cycle step with the highest pressure drop should be downward. All other flows can then be in the same direction as the limiting flow (cocurrent) or in the opposite direction (countercurrent). Each combination of flow directions for heating and cooling produces a different residual of adsorbate (Fig. 13).

Although most applications of fixed beds have multiple adsorber beds to treat continuous streams, batch operation using a single adsorber bed is an alternative. For purification applications, where one vessel can contain enough adsorbent to provide treatment for days, weeks, or even months, the cost savings and simplicity often justify the inconvenience of stopping adsorption treatment periodically for a short regeneration.

When the mass-transfer zone is a major portion of an adsorbent bed, the equilibrium capacity is poorly utilized. A lead-trim configuration uses the adsorbent more fully. The feed flows successively through a lead bed and then a trim bed. The lead bed is nearly exhausted before it is taken out of service to be regenerated. When a lead bed is removed from adsorption, the trim bed becomes the lead, and a fully regenerated bed becomes the new trim bed.

When large flows are to be treated, designing and building a single adsorber vessel large enough to treat the entire stream is not practical. Instead, the feed flow is split equally between parallel beds and/or trains of adsorbers. This provides the additional advantage of a convenient method of turning down the process to save on utilities.

At the start of the cooling step, the adsorber vessel is a large heat sink containing valuable energy: the sum of all of the sensible heats of the adsorbent, the vessel, and any internals. If we use three adsorber beds—one on adsorption, one on heating, and one on cooling—the purge gas flows in series first to cool a hot bed and then to heat a spent bed. Thus all of the heat from the bed being cooled is recovered.

Thermal energy can also be conserved by using a thermal-pulse cycle. When desorption is heat limited, only a short soak time at temperature completes

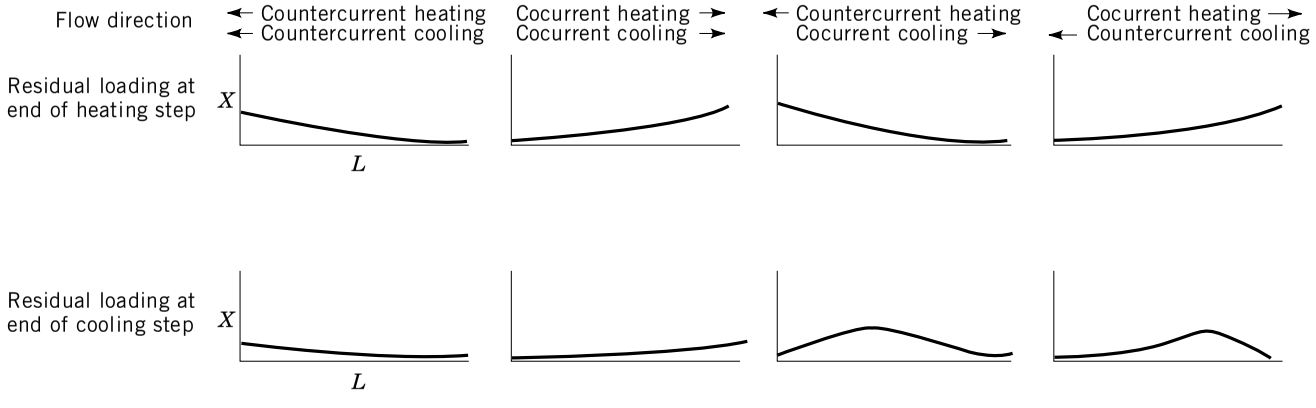

Fig. 13. Shape of residual loading gradient (61). L is bed length. Courtesy of *Chemical Engineering*.

regeneration. The entire adsorbent bed need not be at desorption temperature before beginning the cooling step. Only a pulse of heating gas that contains the heat of desorption is required to move through the bed, desorbing the adsorbate until it exhausts its thermal energy as it reaches the outlet. Because temperature fronts spread as they move through packed beds, a small excess of heat is added to the stoichiometric quantity to ensure that the outlet reaches the desired level before being cooled.

When the gas available for regeneration is in short supply, the regeneration steps are often carried out in a closed loop. This recycle of the bed effluent back to the inlet has the advantage of concentrating the impurity and making it easier to separate by condensation or other recovery means. Heating is usually accomplished with a semiclosed loop that has a constant fresh gas makeup and a bleed to draw off the desorbed material. However, contaminant is at a higher level than in an open loop and product purity is harder to achieve.

Drying. The single most common gas-phase application for TSA is drying. The natural gas, chemical, and cryogenics industries all use zeolites, silica gel, and activated alumina to dry streams.

Zeolites, activated alumina, and silica gel have all been used for drying of pipeline natural gas. Alumina and silica gel have the advantage of having higher equilibrium capacity and of being more easily regenerated with waste level heat (62). However, the much lower dewpoint and longer life attainable with 4A makes zeolites the predominant adsorbent. Special acid-resistant zeolites are used for natural gas containing large amounts of acid gases, such as CO_2 and H_2S.

The low dewpoint that can be achieved with zeolites is especially important when drying feed streams to cryogenic processes to prevent freeze-up at process temperatures. Natural gas is dried before liquefaction to liquefied natural gas (LNG), both in peak demand and in base load facilities. Zeolites have largely replaced silica gel and activated alumina in drying natural gas for ethane recovery utilizing the cryogenic turboexpander process, and for helium recovery. The air to be cryogenically distilled into N_2, O_2, and Ar must be purified of both H_2O and CO_2, and traces of mercury and hydrocarbon to protect the aluminum heat exchangers. This purification is accomplished with 13X zeolites or a compound bed of activated alumina and zeolite.

The 4A zeolite, silica gel, and activated alumina all find applications drying synthesis gas, inert gas, hydrocracker gas, rare gases, and reformer recycle H_2. Cracked gas before low temperature distillation for olefin production is a reactive stream. The 3A or pore-closed 4A zeolite size selectively adsorbs water but excludes the hydrocarbons, thus preventing coking (62). This molecular sieving also prevents coadsorption of hydrocarbons that would otherwise be lost during desorption with the water. Small pore zeolites are also applied to the drying of ethylene, propylene, and acetylene as they are drawn from salt cavern, or conventional, storage. When industrial gases containing Cl_2, SO_2, and HCl are dried, acid-resistant zeolites are used.

A recently developed drying application is the dehumification of air in buildings utilizing desiccant wheels. In an increasingly environmentally conscious world, adsorption is an alternative to the use of vapor compression air conditioning with its high electrical consumption and the potential for release

of harmful refrigerants. In a typical system, the fresh air flows through the rotary dryer is partially cooled in a cross exchanger, and is brought to the desired temperature by an evaporative cooler. Exhaust air is used as a cooling source for the cross-exchanger and is heated by low level energy hot enough to remove the moisture from the desiccant wheel (63). The adsorbent can be silica gel, zeolite, or mixtures (64). The adsorbent can also remove some of the organic contaminants from the outside ambient air. The 5A zeolite was found to be superior to silica gel in removing CO, NO_2, and SO_2 in desiccant service, but more difficult to regenerate (65).

Sweetening. Another significant purification application area for adsorption is sweetening. Hydrogen sulfide, mercaptans, organic sulfides and disulfides, and COS need to be removed to prevent corrosion and catalyst poisoning. They are to be found in H_2, natural gas, deethanizer overhead, and biogas. Often adsorption is attractive because it dries the stream as it sweetens.

In the sweetening of wellhead natural gas to prevent pipeline corrosion, 4A zeolites allow sulfur compound removal without CO_2 removal (to reduce shrinkage), or the removal of both to upgrade low thermal content gas. When minimizing the formation of COS during desulfurization is desirable, bivalent cation-exchanged zeolites are commonly used because they are less catalytically active for the reaction of CO_2 with H_2S to form COS and water. Such calcium-, manganese-, and zinc-exchanged zeolites exhibit reduced reactivity while maintaining H_2S capacity with some loss of mass-transfer rate (66). Natural gas for steam–methane reforming in ammonia production must be sweetened to protect the sulfur sensitive, low-temperature, shift catalyst. Zeolites are better than activated carbon because mercaptans, COS, and organic sulfides are also removed. Many refinery H_2 streams require H_2S and water removal by 4A and 5A zeolites to prevent poisoning of catalysts such as those in catalytic reformers.

Other Separations. Other TSA applications range from CO_2 removal to hydrocarbon separations, and include removal of air pollutants and odors, and purification of streams containing HCl and boron compounds. Because of their high selectivity for CO_2 and their ability to dry concurrently, 4A, 5A, and 13X zeolites are the predominant adsorbents for CO_2 removal by temperature-swing processes. The 4A-type zeolite is used for CO_2 removal from baseload and peak-shaving natural gas liquefaction facilities.

The removal of volatile organic compounds (VOC) from air is most often accomplished by TSA, especially with steam. Air streams needing treatment can be found in most chemical and manufacturing plants, especially those using solvents. At concentrations from 500 to 15,000 ppm, recovery of the VOC from steam used to regenerate activated carbon adsorbent thermally is economically justified, or they may be recovered using PSA (see below). Concentrations $>$15,000 ppm are typically in the explosive range and require the use of inert gas rather than air for regeneration. Below $\sim$500 ppm, recovery is not economically justifiable, but environmental concerns often dictate adsorptive recovery followed by destruction. Activated carbon is the long-established adsorbent for these applications, which represent the second largest use for gas-phase carbons. Hydrophobic adsorbents such as high silica zeolites and macroreticular resins are finding increased useage for VOC. The high silica zeolites can be regenerated by air without the ignition threat posed by activated carbon. This stability allows

VOC destruction with adsorber/oxidizer hybrids systems (67). Honeycomb adsorbent wheels have been fabricated with activated carbon fibers (68), and with high silica zeolites (69). These rotary adsorbent beds reduce utility consumption due to lower pressure drop, reduce adsorbent inventory requirement, and provide continuous operation with nearly constant compositions. Activated carbon cloth has also been incorporated into fixed beds (70) and regenerated electrothermally (57). Wheels have been developed for cabin air cleanup in automobiles and airplanes (71).

A number of inorganic pollutants are removable by TSA processes. One of the major pollutants requiring removal is SO_2 from flue gases and from sulfuric acid plant tail gases. The Sulfacid and Hitachi fixed-bed processes, the Sumitomo and BF moving-bed processes, and the Westvaco fluidized-bed process all use activated carbon adsorbents for proven SO_2 removal (72). Zeolites with high acid resistance, such as mordenite and clinoptilolite, have proven to be effective adsorbents for dry SO_2 removal from sulfuric acid tail gas (73). Hydrophobic zeolite adsorbents (74), pillared interlayered clays (PILCs) (75), and resins (76) have all been shown to work in this application.

Zeolites have also proven applicable for removal of nitrogen oxides (NO_x) from wet nitric acid plant tail gas (73). The removal of NO_x from flue gases can also be accomplished by adsorption. The Unitaka process utilizes activated carbon with a catalyst for reaction of NO_x with ammonia, and activated carbon has been used to convert NO to NO_2, which is removed by scrubbing (72). Mercury is another pollutant that can be removed and recovered by TSA. Activated carbon impregnated with elemental sulfur is effective for removing Hg vapor from air and other gas streams; the Hg can be recovered by *ex situ* thermal oxidation in a retort (77). Mordenite and clinoptilolite zeolites are used to remove HCl from Cl_2, chlorinated hydrocarbons, and reformer catalyst gas streams (78). Activated aluminas are also used for such applications, and for the adsorption of fluorine and boron–fluorine compounds from alkylation (qv) processes.

4.2. Pressure Swing. A PSA cycle is one in which desorption takes place at a pressure much lower than adsorption. Its principal application is for bulk separations where contaminants are present at high concentration. The PSA cycles are characterized by high residual loadings and low operating loadings. Figure 14 shows the operating loading (X_1–X_2) that derives from the partial pressure at feed conditions and the lower pressure P_2 at the end of desorption. These low adsorption capacities for high concentrations mean that cycle times must be short, seconds to minutes, for reasonably sized beds. Fortunately, packed beds of adsorbent respond rapidly to changes in pressure. A purge usually removes the desorbed components from the bed, and the bed is returned to adsorption condition by repressurization. Applications may require additional steps. Systems with weakly adsorbed species are especially suited to PSA adsorption. The applications of PSA include drying, upgrading of H_2 and fuel gases, and air separation. Several broad reviews of PSA have been written (79–82).

Principles. In a PSA cycle, two processes occur during regeneration: depressurizing and purging. Depressurization must provide adequate reduction in the partial pressure of the adsorbates to allow desorption. Enough purge gas must flow through the adsorbent to transfer the desorbed material away. Equilibrium determines the maximum capacity of the gas to accomplish this. These

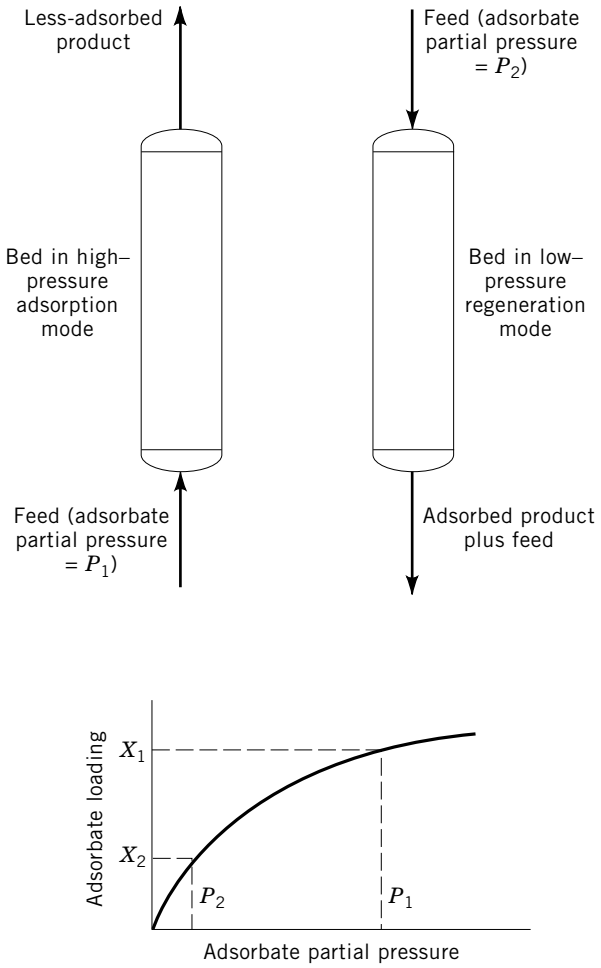

Fig. 14. Pressure-swing cycle (1).

cycles operate at nearly constant temperature and require no heating or cooling steps. They utilize the exothermic heat of adsorption remaining in the adsorbent to supply the endothermic heat of desorption. Pressure-swing cycles are classified as PSA, VSA (vacuum-swing adsorption), PSPP (pressure-swing parametric pumping) or RPSA (rapid pressure-swing adsorption). PSA swings between a high superatmospheric and a low superatmospheric pressure, and VSA swings from a superatmospheric pressure to a subatmospheric pressure. Otherwise, the principles involved are the same.

The other means of accomplishing pressure cycling of an adsorbent is parametric pumping, in which a single adsorbent bed is alternately pressurized with forward flow and depressurized with backward flow through the column from reservoirs at each end. Like TSA parametric pumping, one component concentrates in one reservoir and one in the other. As the name implies, pressure-swing parametric pumping embodies pressure changes that are more than pressuring and depressurizing a bed of adsorbent. Significant pressure gradients

occur in the bed. These gradients are especially critical to the way that RPSA cycles operate and result in much smaller adsorbent beds and simpler processes.

In most applications of adsorption, the separation is carried out by adsorbing the more strongly adsorbed species from the less strongly adsorbed. These separations are thus equilibrium limited. However, an adsorptive separation can also be based on a rate or kinetically limited system. Slightly larger molecules diffuse more slowly through a microporous adsorbent with properly selected pore diameter. Therefore, in a rapidly cycling process such as PSA, smaller molecules can be preferentially adsorbed even in the absence of any equilibrium selectivity.

Steps. A PSA cycle has at least three steps: adsorption, blowdown, and repressurization. Although not always necessary, a purge step is normally used. In finely tuned processes, cocurrent depressurization and pressure-equalization steps are frequently added.

At the completion of adsorption, the less selectively adsorbed components have been recovered as product. However, a significant quantity of the weakly adsorbed species are held up in the bed, especially in the void spaces. A cocurrent depressurization step reduces the bed pressure by allowing flow out of the bed cocurrently to feed flow and thus reduces the amount of product retained in the voids (holdup), improving product recovery, and increases the concentration of the more strongly adsorbed components in the bed. The purity of the more selectively adsorbed species has been shown to depend strongly on the cocurrent depressurization step for some applications (83). A cocurrent depressurization step is optional because a countercurrent one always exists. Criteria have been developed to indicate when the use of both is justified (84).

None of the selectively adsorbed components is removed from the adsorption vessel until the countercurrent depressurization (blowdown) step. During this step, the strongly adsorbed species are desorbed and recovered at the adsorption inlet of the bed. The reduction in pressure also reduces the amount of gas in the bed. By extending the blowdown with a vacuum (ie, VSA), the productivity of the cycle can be greatly increased.

Additional stripping of the adsorbates from the adsorbent and purging of them from the voids is accomplished by the purge step. This step can occur concurrently with the end of the blowdown or be carried out afterward. This step is accomplished with a flow of product into the product end to provide a low residual of the selectively adsorbed components at the effluent end of the bed. Although the purge can be done at the same temperature as adsorption, raising the temperature can achieve better desorption and is sometimes used; such cycles are actually a hybrid of PSA and TSA referred to as PTSA. Because PSA cycles are shorter than those of TSA, a thermal assist of PSA does not gain as much as a vacuum assist of TSA.

The repressurization step returns the adsorber to feed pressure and completes the steps of a PSA cycle. Pressurization is carried out with product and/or feed. Pressurizing with product is done countercurrent to adsorption so that purging of the product end continues; indeed it may be merely a continuation of the purge step but with the bed exit valve closed. Pressurizing with feed cocurrent to adsorption in effect begins adsorption without producing any product.

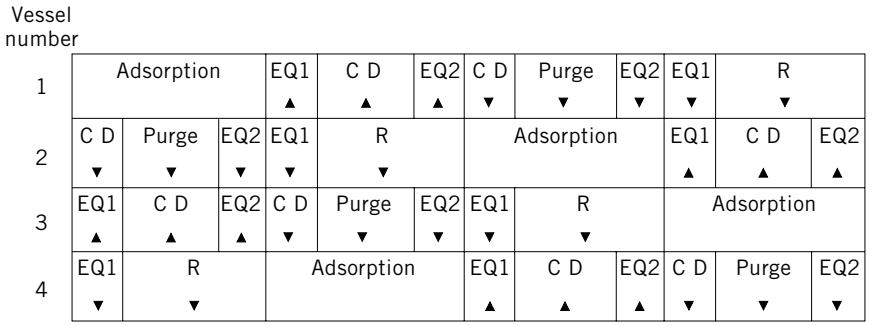

Fig. 15. Four-bed PSA system cycle sequence chart (82). EQ, equalization; C D ▲, cocurrent depressurization; C D ▼, countercurrent depressurization; R, repressurization; ▲, cocurrent flow; ▼, countercurrent flow. Courtesy of American Institute of Chemical Engineers.

Pressure equalization steps are used to conserve gas and compression energy. They are applied to reduce the quantity of feed or product gas needed to pressurize the beds. Portions of the effluent gas during depressurization, blowdown, and purge can be used for repressurization.

Flow Sheet. The most common processing scheme has two or three fixed-bed adsorbers alternating between the adsorption step and the desorption steps. The simplest two-bed configuration is illustrated in Figure 14. However, the variations possible to achieve special separations are endless. Single beds with external surge vessels provide continuous flow; multiple beds are used to accommodate additional steps. An example of the bed sequencing needed for multiple steps in a four-bed PSA is shown in Figure 15. Beds can be configured in series or parallel to accomplish coproduction. The UOP Polybed PSA system uses five to ten beds to maximize the recovery of the less selectively adsorbed component and to extend the process to larger capacities (85).

The flow directions in a PSA process are fixed by the composition of the stream. The most common configuration is for adsorption to take place upflow. All gases with compositions rich in adsorbate are introduced into the adsorption inlet end, and so effluent streams from the inlet end are rich in adsorbate. Similarly, adsorbate-lean streams to be used for purging or repressurizing must flow into the product end.

Because RPSA is applied to gain maximum product rate from minimum adsorbent, single beds are the norm. In such cycles where the steps take only a few seconds, flows to and from the bed are discontinuous. Therefore, surge vessels are usually used on feed and product streams to provide uninterrupted flow. Some RPSA cycles incorporate delay steps unique to these processes. During these steps, the adsorbent bed is completely isolated; and any pressure gradient is allowed to dissipate (86).

Purifications. The major purification applications for PSA are for hydrogen, methane, and drying. One of the first commercial uses was for gas drying in which the original two-bed Skarstrom cycle was used. This cycle uses adsorption, countercurrent blowdown, countercurrent purge, and cocurrent

repressurization to produce a dry air stream with <1 ppm H_2O (87). About one half of all dryers of instrument air use a PSA cycle similar to this one, most commonly using activated alumina or silica gel (88). Zeolites are used to obtain the lowest possible dewpoints. Some applications for drying air do not require a low level of H_2O, but only a significant lowering of the dew point. The pneumatic compressor systems used in vehicle air-brakes are an example; when a 10–30 K dew point depression is needed for higher discharge air temperatures in the presence of compressor oil, zeolites have been demonstrated to have an advantage over activated alumina and silica gel (89).

High purity H_2 is needed for applications such as hydrogenation, hydrocracking, and ammonia and methanol production. As a significant source of such gas, PSA is able to produce purities as high as 99.9999% using technologies such as the UOP Polybed approach (85). Most H_2 purification by PSA is associated with steam reforming of natural gas and with ethylene-plant and refinery off-gas streams. Hydrogen is also available in coke-oven gas, cracked ammonia, and coal-gasification gas. The contaminants that have to be removed by PSA include carbon oxides, N_2, O_2, Ar, NH_3, CH_4, and heavier hydrocarbons. To remove these components, adsorbent beds are compounded of activated carbon, zeolites, and carbon molecular sieves.

PSA can also be used to recover VOC from exhaust streams and from gasoline storage and loading facilities. Dow Chemical markets such systems using beads of activated carbon or resin under the trade name SORBATHENE (90).

Bulk Separations. Air separation, methane enrichment, and iso-/normal separations are the principal bulk separations for PSA. Others are the recovery of CO and CO_2.

The PSA process is used to separate air into N_2 and O_2. Many companies market systems for PSA O_2; zeolites 5A, 13X, clinoptilolite and mordenite, and carbon molecular sieves are commonly used in PSA, VSA, and RPSA cycles. The product purity ranges from 85 to 95% (limited by the argon, which normally remains with the O_2). The majority of this O_2 is employed for electric furnace steel, with lesser amounts for waste water treating and solid waste and kilns. Smaller production units, especially those based on RPSA cycles, are used for patients requiring respiratory inhalation therapy in the hospital and at home and for pilots on board aircraft. Enriched air, 25–55% O_2, used to enhance combustion, chemical reactions, and ozone production can be produced by tuning PSA processes.

Although air depleted in oxygen can be produced by an equilibrium-limited PSA, most PSA systems to produce N_2 are based on kinetic PSA. High purity, up to 99.99%, N_2 is produced when rate-limited PSA preferentially adsorbs oxygen from air on A-type zeolites or carbon molecular sieve even though the equilibrium selectivity favors N_2 (91). The major use for such N_2 is inert blanketing, such as in metal heat-treating furnaces; small units are used to purge aircraft fuel tanks and in the food and beverage industry.

The upgrading of methane natural gas pipeline quality is another significant PSA separation area. When high nitrogen causes the natural gas to be of poor quality, kinetic PSA is used to increase the energy content. The diffusion rate of nitrogen into clinoptilolite is several orders of magnitude faster than methane (92).

Methane is recovered from fermentation gases of landfills and wastewater purification plants and from poor-quality natural gas wells and tertiary oil recovery when CO_2 is the major bulk contaminant. Fermentation gases are saturated with water and contain "garbage" components such as sulfur and halogen compounds, alkanes, and aromatics. These impurities must first be removed by TSA using activated carbon or carbon molecular sieves. The CO_2 is then selectively adsorbed in a PSA cycle using either zeolites or silica gel in an equilibrium separation (93). Or, because the diffusivity for CO_2 is $\sim$200 times that of CH_4 on a properly selected carbon molecular sieve, the separation can be made in a kinetic-assisted equilibrium separation (94).

4.3. Purge Swing. A purge-swing adsorption cycle is one in which desorption takes place at the same temperature and total pressure as adsorption. Regeneration is accomplished either by partial-pressure reduction by an inert gas purge or by adsorbate displacement by an adsorbable gas. Its major application is for bulk separations when contaminants are at high concentration. Like PSA, purge cycles are characterized by high residual loadings, low operating loadings, and short cycle times (minutes). Mixtures of weakly adsorbed components are especially suited to purge-swing adsorption. Applications include the separation of normal from branched and cyclic hydrocarbons, and for gasoline vapor recovery.

Principles. Purging must provide adequate reduction in the partial pressure of the adsorbates to allow desorption. With enough purge volume, loadings as high as the loading X_1 in equilibrium with the feed partial pressure P_1 can be achieved, as shown in Figure 16. Reduction in partial pressure operates analogously to the reduction in system pressure in PSA cycles. Equilibrium determines the maximum capacity of the gas to purge the adsorbate. These cycles operate adiabatically at nearly constant inlet temperature and require no heating or cooling steps. As with PSA, purge processes utilize the exothermic heat of adsorption remaining in the adsorbent to supply the endothermic heat of desorption. Purge cycles are divided into two categories, inert purge and displacement purge. In inert-purge stripping, inert refers to the fact that the purge gas is not appreciably adsorbable at the cycle conditions. Inert purging desorbs the adsorbate solely by partial pressure reduction.

In displacement-purge stripping, displacement refers to the displacing action of the purge gas caused by its ability to adsorb at the cycle conditions. This competitive adsorption tends to desorb the adsorbate in addition to the partial pressure reduction of dilution. Displacement purging is not as dependent on the heat of adsorption remaining on the adsorbent, because the adsorption of purge gas can release much or all of the energy needed to desorb the adsorbate. The adsorbate must be more selectively adsorbed than the displacement purge so that it can desorb purge fluid during the adsorption step. The displacement purge gas composition must be carefully selected, because it contaminates both the product stream and the recovered adsorbate and requires distillation as illustrated in Figure 17. The displacement purge is more efficient for less selective adsorbate–adsorbent systems; systems with high equilibrium loading of adsorbate require more purging (95).

Steps. A purge-swing cycle usually has two steps: adsorption and purge. Sometimes, a cocurrent purge is added. After the adsorption step has been

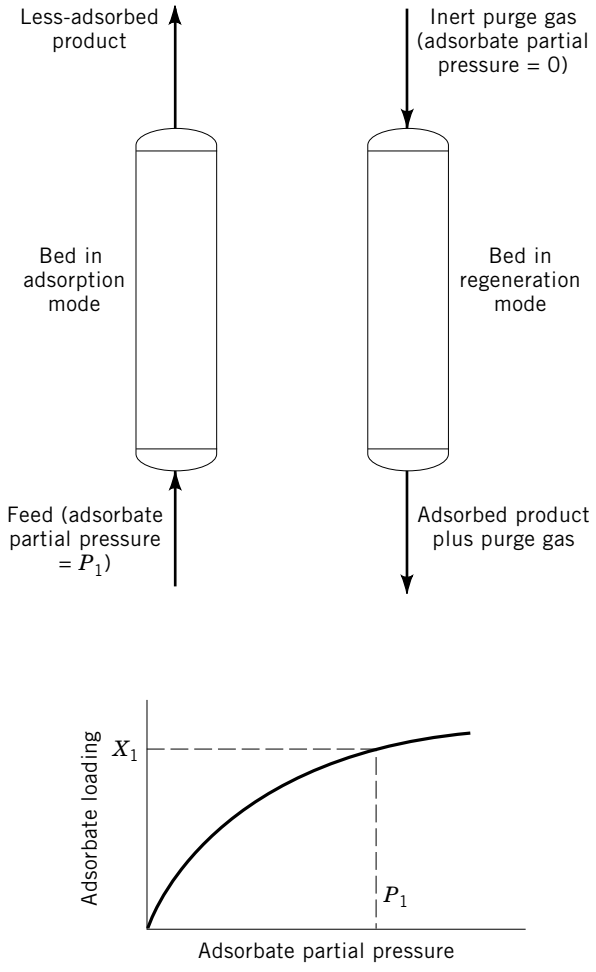

Fig. 16. Inert-purge cycle (1).

completed and the less selectively adsorbed components have been recovered, an appreciable amount of product is still stored in the bed. A purge cocurrent to feed can increase recovery by displacing the fluid held in the voids.

The more selectively adsorbed components are stripped from the adsorbent bed during the countercurrent purge step. By purging into the product end of the bed, a lower residual loading of the selectively adsorbed species can be achieved in the portion of the adsorber that determines product quality.

Flow Sheet. Most purge-swing applications use two fixed-bed adsorbers to provide a continuous flow of feed and product (Fig. 16). Single beds are used when the flow to be treated is intermittent or cyclic. Because the purge flow is invariably greater than the total feed treated, purge is carried out in the down-flow direction to prevent bed lifting, and adsorption is up-flow.

Applications. Several purge-swing processes for the separation of C10–C18 iso- from normal paraffins have been commercialized: Exxon's Ensorb,

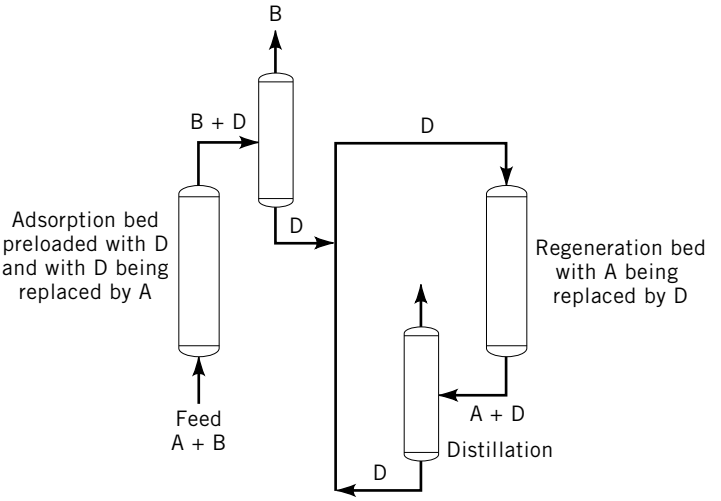

Fig. 17. Displacement-purge cycle (1).

Texaco Selective Finishing (TSF), Leuna Werke's Parex, and the Shell Process (62). All of these processes take advantage of the molecular size selectivity of 5A zeolite, but vary in the purge fluid. Ammonia is used in a displacement-purge cycle in Ensorb. Normal paraffins or light naphtha with a carbon number of two to four less than the feed stream are used for the displacement purge for TSF, Parex, and the Shell Process (96). Since 1971 all U.S. automobile models must have canisters of activated carbon to control gasoline vapors. Any gasoline vapors from the carburetor or the gas tank during running, from the tank during diurnal cycling, and from carburetor hot-soak losses are adsorbed by the carbon and held until they can be regenerated. The vapors are desorbed by an inert purge of air and are drawn into the carburetor as fuel when the engine is running (97). This gas-phase use for activated carbon is the third largest after solvent recovery and air purification.

4.4. Nonregenerative Processing. Gas-phase adsorption can also be used when regenerating the adsorbent is not practical. Most of these applications are used where the facilities to effect a regeneration are not justified by the small amount of adsorbent in a single unit. Nonregenerative adsorbents are used in packaging, dual-pane windows, odor removal, and toxic chemical protection.

Applications. Silica gel is the adsorbent most commonly used as a desiccant in packaging. Activated carbon is used in packaging and storage to adsorb other chemicals for preventing the tarnishing of silver, retarding the ripening or spoiling of fruits, "gettering" (scavenging) outgassed solvents from electronic components, and removing odors.

Adsorbents are used in dual-pane windows to prevent fogging between the sealed panes that could result from the condensation of water or the solvents used in the sealants. Synthetic zeolites (3A, 4A, 13X) or, less frequently, blends of zeolites with silica gel are installed in the spacing strips in double-glazed windows to adsorb water during initial dry-down and any in-leakage and to

adsorb organic solvents emitted from the sealants during their cure. The adsorbent or mix of adsorbents applied depends on the sealant system and filling gas used.

The largest use of activated carbon is for the purification of air streams. Much of this carbon is used to treat recirculated air in large occupied enclosures, such as office buildings, apartments, and plants. The carbon is incorporated into thin filter-like frames to treat the large volumes of air with low pressure drop. Odors are also removed from smaller areas by activated carbon filters in kitchen hoods, air conditioners, and electronic air purifiers. On a smaller scale, gas masks containing carbon or carbon impregnated with promoters are used to protect wearers from odors and toxic chemicals. The smallest scale carbon filters are those used in cigarettes. In addition to protection from hazardous chemicals in industry, activated carbon gas masks can protect against gas-warfare chemicals. Activated carbon fibers have been formed into fabrics for clothing to protect against vesicant and percutaneous chemical vapors.

4.5. Reactive Adsorption. Although chemisorbents are not used as extensively as physical adsorbents, a number of commercially significant processes employ chemisorption for gas purification.

Desulfurization. An old method for removal of sulfur compounds involves contacting gases containing H_2S and H_2O with α- or γ-ferric oxide monohydrates at $\sim 38^{\circ}C$ to adsorb the sulfur in the form of ferric sulfide, followed by periodic reoxidation of the surface to form elemental sulfur and to "revivify" the ferric oxides (98). The iron sponge is reused in this cycle until buildup of sulfur in its pores reduces its effectiveness and it is replaced with fresh adsorbent. The process is most efficient when the treated gases contain oxygen to allow continuous revivification. Spent adsorbents may be regenerated, e.g., by oxidation of the sulfur to SO_2 to be fed to a sulfuric acid plant or by solvent extraction with carbon disulfide, and reused.

When activated carbon is used to adsorb H_2S from air it undergoes similar reactions. Regeneration can be accomplished with water to form sulfuric acid (99), or with heated air to form SO_2 (100).

Mercury Removal. Trace amounts of mercury found in natural gas in some parts of the world are known to cause significant pinhole corrosion damage to aluminum heat exchanger surfaces in cryogenic coldboxes upstream of liquefied natural gas LNG plants. Mercury can be removed from such streams, and other industrial gases, down to low concentrations by treatment in an *ex situ* TSA regenerative process using an activated carbon adsorbent containing sulfur, and allowing reactions involving the formation of mercuric sulfide to remove mercury from the gas. Alternatively, the mercury can be removed by a newly developed adsorbent that may be employed in either nonregenerative or TSA regenerative process cycles (101).

Nuclear Waste Management. Separation of radioactive wastes provides a number of relatively small scale but vitally important uses of gas-phase purification applications of adsorption. Such applications often require extremely high degrees of purification because of the high toxicity of many radioactive elements.

Delay for Decay. Nuclear power plants generate radioactive xenon and krypton as products of the fission reactions. Although these products are trapped inside the fuel elements, portions can leak out into the coolant (through fuel

cladding defects) and can be released to the atmosphere with other gases through an air ejector at the main condenser.

To prevent such release, off gases are treated in Charcoal Delay Systems, which delay the release of xenon and krypton, and other radioactive gases, such as iodine and methyl iodide, until sufficient time has elapsed for the short-lived radioactivity to decay. The delay time is increased by increasing the mass of adsorbent and by lowering the temperature and humidity; for a boiling water reactor (BWR), a typical system containing 21 t of activated carbon operated at 255 K, at 500 K dewpoint, and 101 kPa (15 psia) would provide ~42 days holdup for xenon and 1.8 days holdup for krypton (102). Humidity reduction is typically provided by a combination of a cooler-condenser and a molecular sieve adsorbent bed.

If the spent fuel is processed in a nuclear fuel reprocessing plant, the radioactive iodine species (elemental iodine and methyl iodide) trapped in the spent fuel elements are ultimately released into dissolver off gases. The radioactive iodine may then be captured by chemisorption on molecular sieve zeolites containing silver (103).

Other Applications. Many applications of adsorption involving radioactive compounds simply parallel similar applications involving the same compounds in nonradioactive forms, eg, radioactive carbon-14, or deuterium- or tritium-containing versions of CO_2, H_2O, hydrocarbons. For example, molecular sieve zeolites are commonly employed for these separations, just as for the corresponding nonradioactive uses.

4.6. Moving/Fluidized Beds and Wheels. Most adsorption systems use stationary-bed adsorbers. However, efforts have been made over the years to develop moving-bed adsorption processes in which the adsorbent is moved from an adsorption chamber to another chamber for regeneration, with countercurrent contacting of gases with the adsorbents in each chamber. Union Oil's Hypersorption Process (104) is an example. However, this process proved uneconomical, primarily because of excessive losses resulting from adsorbent attrition.

The commercialization by Kureha Chemical Co. of Japan of a new, highly attrition-resistant, activated-carbon adsorbent as Beaded Activated Carbon (BAC) allowed development of a process employing fluidized-bed adsorption and moving-bed desorption for removal of volatile organic carbon compounds from air. The process has been marketed as GASTAK in Japan and is now marketed as SOLDACS by Daikin Industries, Ltd; such a system is offered in the United States by Carbon Resources. Nobel Chematur has developed a similar system based on resin beads marketed in the United States by American Purification and by Weatherly.

Another application for moving beds is in the treatment of flue or exhaust gases. Here the adsorbent flows downward in a cross-flow mode to minimize pressure drop. Copper oxide on alumina was used in such a configuration to remove SO_2 and NO_x (105), activated carbon to adsorb SO_2 (72), and activated carbon to remove VOC (106).

Recently wheels have been commercialized for ambient pressure applications in order to reduce costly pressure drop. Their major application has been TSA cycles for drying and for VOC removal (see above).

5. Design Methods

Design techniques for gas-phase adsorption range from empirical to theoretical, from simple to computationally intensive. Methods have been developed for equilibrium, mass transfer, and combined dynamic performance. Approaches are available for the regeneration methods of heating, purging, steaming, and pressure swing. Many tools exist to aid the adsorption system designer. Computer-based models have been presented in the literature, and AspenTech offers one commercially trademarked ADSIM, which includes the most popular equilibrium models, as well as allowing user-defined ones, ADSIM has modules for unsteady-state simulation to examine control strategies. ProSim has an adsorption column model in its ProSimPlus software based on (39,107,108). Several broad reviews have been published on analytical equations describing adsorption (109), on experimental adsorption equilibrium and kinetic data (110,111), on theoretical models for adsorption processes (112,113), on adsorption design considerations (1,114,115), and on molecular modeling (116). An extensive bibliographic listing of adsorption (and other separation processes) is maintained at, and available by subscription from, the School of Chemical Engineering, Curtin University of Technology, Perth, Australia (117).

5.1. Adsorption. In the design of the adsorption step of gas-phase processes, two phenomena must be considered: equilibrium and mass transfer. Sometimes adsorption equilibrium can be regarded as that of a single component, but more often several components and their interactions must be accounted for. Design techniques for each phenomenon exist as well as some combined models for dynamic performance.

Equilibrium. Among the aspects of adsorption, equilibrium is the most studied and published. Many different adsorption equilibrium equations are used for the gas phase; the more important have been presented (see the section on Isotherm Models). Equally important is the adsorbed phase mixing rule that is used with these other models to predict multicomponent behavior.

Many simple systems that could be expected to form ideal liquid mixtures are reasonably predicted by extending pure-species adsorption equilibrium data to a multicomponent equation. The potential theory has been extended to binary mixtures of several hydrocarbons on activated carbon by assuming an ideal mixture, and to O_2 and N_2 on 5A and 10X zeolites (118,119). Mixture isotherms predicted by IAST agree with experimental data for methane + ethane and for ethylene + CO_2 on activated carbon, and for $CO + O_2$ and for propane + propylene on silica gel (39). A statistical thermodynamic model has been successfully applied to equilibrium isotherms of several nonpolar species on 5A zeolite, to predict multicomponent sorption equilibria from the Henry constants for the pure components (29). A set of equations that incorporate surface heterogeneity into the IAST model (HIAST) provides a means for predicting near-ideal multicomponent equilibria (120).

For most models of adsorptive equilibrium, however, the coefficients derived from pure species are not adequate to predict multicomponent equilibrium for nonideal mixtures. Fitting the systems ethane + ethylene + propane on 5A zeolite and H_2S + CO_2 on H-mordenite required using binary parameters with the IAST or the real adsorbed solution theory models (121). A coalescing

factor applied to the potential theory did collapse all isotherms to a single curve for activated carbon, zeolites, and silica gel. A binary interaction parameter that is a function of the coalescing factor was needed to gain agreement with binary data (122). For the multicomponent system of H_2, CO, CH_4, CO_2, and H_2S on activated carbon, an interaction parameter was required in the extended Langmuir equation to predict multicomponent equilibrium (123). Cross-correlation coefficients were necessary to apply a statistical model to three nonideal ternary zeolite systems (124). An activity coefficient whose composition dependence is described by the Wilson equation has been added to the VSM to fit data for hydrocarbons on activated carbon and $O_2 + N_2$ on 10X zeolite (40). Activity coefficients of the adsorbate–adsorbate interactions, or treatment of the surface as heterogeneous, are correlative methods that allow extension of the IAST to binary adsorption (125). Several models were tested with the addition of activity coefficients for the nonideal systems CO_2, ethylene and ethane on 5A zeolite, and carbon molecular sieve (126). A two-dimensional virial equation of state was needed to predict nonideal equilibrium of CO_2, H_2S and propane on H-mordenite and *n*-hexane and water on activated carbon (127).

Mass Transfer. The degree of approach to equilibrium that can be achieved in adsorption is determined by the mass-transfer rates. One useful design concept is the mass-transfer zone (MTZ), an extension of the ion-exchange zone method (128). Figure 18**b** is a depiction of the adsorbate loading in a fixed bed during adsorption. The ordinate is loading (X) and the abscissa is distance (L) from the inlet of the bed. Between the inlet and the exhaustion point (L_e), the loading is in equilibrium with the feed gas, and this section is called the equilibrium section. From the breakthrough point (L_b) to the outlet of the bed, the adsorbate loading is still at the residual loading level and is unused bed. Mass transfer between the gas and the adsorbent is occurring between the breakthrough and exhaustion points, and so this zone is called the MTZ. The length of the bed, L_b to L_e, is called the mass-transfer zone length (MTZL). The MTZL is usually correlated to flow rate or flow velocity (129).

Most dynamic adsorption data are obtained in the form of outlet concentrations as a function of time as shown in Figure 18**a**. The area iebai measures the removal of the adsorbate, as would the stoichiometric area idcai, and is used to calculate equilibrium loading. For constant pattern adsorption, the breakthrough time (Θ_b), and the stoichiometric time (Θ_s), are used to calculate LUB as $(1 - \Theta_b/\Theta_s)L_{\text{bed}}$ (130). This LUB concept is commonly used for drying and desulfurization design in the natural gas industry and for air prepurification before cryogenic distillation.

Another way of subdividing the bed is illustrated in Figure 18**b**. If the mass-transfer resistance were negligible, the MTZ would become a square or stoichiometric front along the line dsc. The area febgf represents used adsorbent loading, while the area ehbe between the potential loading and the actual loading curve eb is unused. By material balance, the area fdcgf up to the stoichiometric front would also represent the used capacity. Therefore, areas febgf and fdegf are equal. This portion of the bed up to the stoichiometric point, s, is called the weight of equivalent equilibrium section (WES). The rest of the adsorbent from the stoichiometric point to the breakthrough point is termed the weight of unused bed (WUB), because it is equivalent to a bed with no usable capacity in

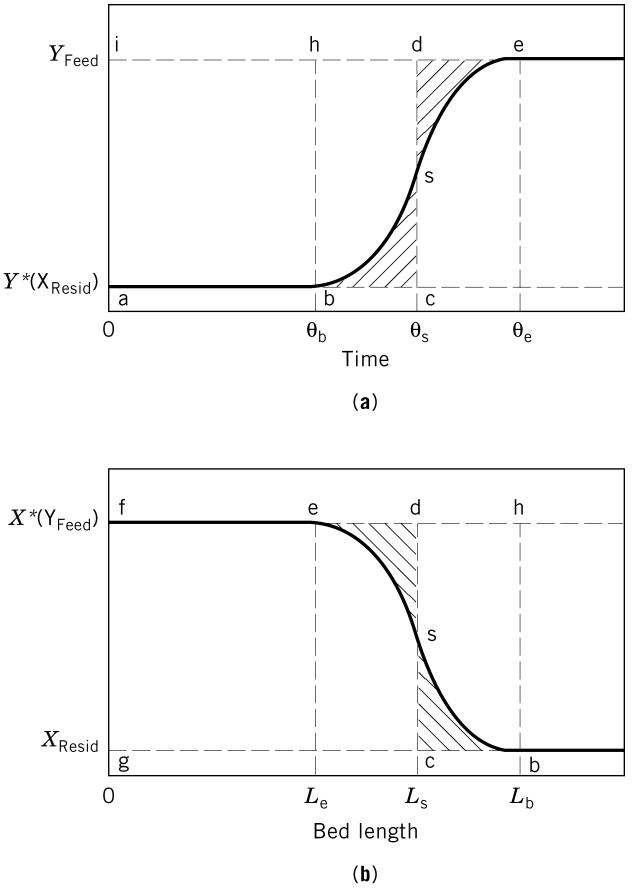

Fig. 18. (**a**) Time trace of adsorbate composition in an adsorber effluent during adsorption. (**b**) Adsorbate loading along the flow axis of an adsorber during adsorption (1).

the stoichiometric interpretation. Adsorption beds can thus be sized by combining a WES calculated from equilibrium data and a WUB derived from kinetic data.

MTZs can be designed by the HTU/NTU mass-transfer concept used in countercurrent liquid/liquid and gas/liquid absorption (131). When this technique is used, it has been found that the mass transfer (HTU) can be uncoupled from the axial dispersion (131). Theoretical stages form the essence of the discrete cell model graphical procedures, which are applied to flat isotherms and incorporate pore diffusivity and axial dispersion.

Dynamic Performance. More complex models do not attempt to separate the equilibrium behavior from the mass-transfer behavior. Rather they treat adsorption as one dynamic process with an overall dynamic response of the adsorbent bed to the feed stream. Although numerical solutions can be attempted for the rigorous partial differential equations, simplifying assumptions are often made to yield more manageable calculating techniques. For systems with a large number of components, the design can be simplified by combining the adsorbates

into pseudospecies based on Freundlich exponent and on mass-transfer coefficients (133).

The *J*-function is a definite integral of an expression including I_0, the modified Bessel function of the first kind. *J*-function curves use stoichiometric time and the number of theoretical stages as the two parameters to fit breakthrough curves and extend to other conditions. These curves have been approximated for use on PC microcomputers (134). A phenomenological model requires the determination of two parameters, a transfer coefficient, and a linear isotherm constant, from a complete breakthrough curve. The solution to the model is in an infinite series form, which is calculable by a hand-held calculator or personal computer (135). Another method separates the equilibrium from the kinetic effects by constructing effective equilibrium curves. Because the solution to the model involves nonlinear algebraic or differential equations, graphs called solution charts are used to predict breakthrough fronts (136). Another solution technique is the use of fast Fourier transforms. Linear isotherms are required, but their applicability for predicting breakthrough curves has been demonstrated for isothermal and nonisothermal adsorbers (137). Another model, with a solution in infinite series form, incorporates separate mass-transfer coefficients for external film, macropore, and micropore resistances (138). Techniques have also been developed to predict breakthrough from fluidized beds. The behavior of organic solvents adsorbed from air on activated carbon was shown to exhibit breakthrough times that can be correlated to the adsorption capacity and the amount of bed expansion (139).

Some specific design methods have been developed for particular applications. Several procedures have been published for the design of gas dryers. The *J*-function has been applied to silica gel dryers after a correlated correction factor accounted for the nonisothermality (140). In other work on drying with activated alumina and silica gel, constant-pattern LUBs were shown applicable for designs at H_2O contents of <0.003 kg/kg air (141). Equilibrium and kinetic parameters for H_2O on activated alumina were determined for a more rigorous nonisothermal model that predicted adiabatic behavior (142). Breakthrough times for several organic vapors on activated carbon respirator cartridges have been found to be predictable by using a theory of statistical moments. In one study, equilibrium data was correlated by the Potential Theory and breakthrough was calculated using the normal probability distribution curve (143). In another, the equilibrium data was represented by a Freundlich equation (144). For heavy hydrocarbon recovery from natural gas on silica gel, the equilibrium data were fit to a Freundlich isotherm and the breakthrough composition was found to have a power dependence on the extent of adsorptive saturation of the adsorbent (137). A WUB design approach was found to predict breakthrough for several organics on activated carbon using a Potential Theory equilibrium curve (145). Correlations of equilibrium capacity and WUB were also found applicable in the removal of H_2S from natural gas using 5A zeolite (146).

5.2. Regeneration. In recent years, considerable effort has been expended to better understand and quantify the process of regeneration. Methods are available to predict thermal, purge, and steaming requirements. Models are available to simulate all of the regeneration types, temperature, pressure, and purge swings (115).

Thermal Requirements. When a TSA cycle is heating limited, the regeneration design is only concerned with transferring energy to the system. Charts for isothermal, linear-isotherm adsorption that were derived by Hougen and Marshall (147) from earlier work on heat transfer from a gas to fixed beds (148) can be reapplied to heat transfer for heating-limited regeneration when the heat of adsorption is negligible (61). This approach has been expanded to include both a correction of one dimensionless time per dimensionless bed length for heat losses and another correction particular to the H_2O–4A zeolite system studied (149). Because cooling is a heating-limited step, it can be calculated by the modified Hougen and Marshall method. As mentioned in the discussion of thermal swing, the cooling step can be performed under some process conditions by starting adsorption with a hot adsorbent; performance is not affected.

Purge Requirements. The amount of purge gas needed in stripping-limited regeneration is similar to that for purge regeneration, but it differs primarily in the temperature at which the isothermal desorption occurs. For a pressure-swing process, the theoretical minimum volumetric purge/feed ratio is the ratio of the purge pressure to the feed pressure (61), and one model shows the optimum ratio to be the minimum purge volume that can be used with the given cyclic steady-state conditions (150). For a thermal-swing process, the minimum purge/adsorbent ratio is the ratio of the heat capacity of the solid to that of the gas (151). Specific design purge data have been published for purge-swing activated-carbon automotive evaporative emissions control (97) and for pressure-swing drying of pneumatic system air (89). The pneumatic system process exhibits an optimum purge ratio for maximizing the attainable dewpoint depression. An isothermal purge-swing model that uses Langmuir equilibrium to simulate adsorbent performance has been presented (152).

Steaming Requirements. The steaming of fixed beds of activated carbon is a combination of thermal swing and displacement purge swing. The exothermic heat released when the water adsorbs from the vapor phase is much higher than is possible with heated gas purging. This cycle has been successfully modeled by equilibrium theory (153).

Temperature Swing. Several fairly comprehensive reviews of thermal-swing adsorption models are found in the literature (107,110,154). Many of these models have been used to carry out parametric analyses with a goal of energy minimization. A nonisothermal model for single components using equilibrium theory demonstrated that efficiency improves with increased purge contact time and high heat capacity purge gas but is minimally affected by initial bed loading (155), and the model defined conditions under which the desorption can be continued with a cold stream without additional overall purge gas. That work also introduced the concept that minimum thermal energy is required at the characteristic temperature, that temperature at which the slope of the equilibrium isotherm is equal to the ratio of the heat capacity at the adsorbent to that of the purge gas. A nonequilibrium, mechanistic model with a multicomponent VSM model of equilibrium (156) and a nonequilibrium nonadiabatic computer model with a Langmuir-like isotherm (107) reached similar conclusions on optimization. Another nonequilibrium nonadiabatic computer model with an Antoine equation isotherm was used with supporting data to demonstrate that significant energy can be saved by proper timing of the cooling step (157). Most modeling

has assumed that the purge gas is clean even though solvent recovery processes use a recirculated stream when an inert purge gas is employed. Using the method of characteristics and a Freundlich isotherm, an equilibrium theory modeled the incorporation of closed-loop heating and cooling steps (158).

Pressure Swing. Design equations have been developed to predict temperature rise, minimum bed length to retain the heat front, minimum purge rate, and effluent composition (159). A nonequilibrium, nonisothermal simulation program with a Freundlich isotherm equation was found to agree with data for drying with silica gel (160). A somewhat simpler isothermal model using an isotherm approximated by two straight lines successfully calculated the volumetric purge/feed ratio needed to achieve varying product dryness using silica gel (161). An adiabatic equilibrium model with a Langmuir isotherm was used to study the blowdown step of a cycle removing CO_2 on activated carbon and 5A zeolite (162). Changing to an isothermal assumption introduced significant errors into the results. The countercurrent pressurization step was investigated with an isothermal equilibrium model using a Langmuir isotherm for O_2 production from air with 5A zeolite (163). The model predicted the dependence of O_2 concentration on countercurrent pressure and was used to study other parameters. An isothermal model with linear isotherms and component-specific pore diffusivity was used and compared to data for the kinetic-limited separation of air by RS-10 zeolite (164). The simulations agreed well with the experimental parametric studies of time and pressure of feed, blowdown, purge, and pressurization. An equilibrium model was formulated to simulate RPSA using a Freundlich isotherm for separation of N_2 and CH_4 (165). Pressure responses, flow rates, and compositions compared favorably as a function of feed pressure, cycle frequency, and product rate. A nonequilibrium, nonisothermal model for RPSA was developed using a linear isotherm and Darcy's law for pressure drop (166). The model predicted performance in agreement with previous data for air separation on 5A zeolite.

5.3. Pressure Drop. The prediction of pressure drop in fixed beds of adsorbent particles is important. When the pressure loss is too high, costly compression may be increased, adsorbent may be fluidized and subject to attrition, or the excessive force may crush the particles. As discussed previously, RPSA relies on pressure drop for separation. Because of the cyclic nature of adsorption processes, pressure drop must be calculated for each of the steps of the cycle. The most commonly used pressure drop equations for fixed beds of adsorbent are those of Ergun (167), Leva (108), and Brownell and co-workers (168). Each of these correlations uses a particle Reynolds number ($\mathrm{Re} = D_\mathrm{p}\mathrm{G}/\mu$) and friction factor ($f$) to calculate the pressure drop (ΔP) per unit length (L) by the equation

$$\frac{\Delta P}{L} = \frac{fG^2}{2g_\mathrm{c}D_\mathrm{p}\rho}$$

where D_p is the particle diameter, G the mass flux, μ the gas viscosity, and ρ the gas density. The methods differ in their definition of D_p and f. For up-flow in fixed-bed adsorbers, fluidization occurs when the pressure drop just balances

the weight, corrected by any buoyancy:

$$\frac{\Delta P}{L} = \frac{(1-\epsilon)\,(\rho_s - \rho)g}{g_c}$$

where ρ_s is the density of the solid. For down-flow in packed beds, the potential for crushing the adsorbent must be checked. Two forces act to crush the particles, pressure drop and the weight of the bed. The sum of these two $(\Delta P + (1-\varepsilon)\rho_s L)$ should be kept less than that which is known to cause adsorbent damage.

6. Future Directions

Advances in fundamental knowledge of adsorption equilibrium and mass transfer will enable further optimization of the performance of existing adsorbent types. Continuing discoveries of new adsorbent materials will also provide adsorbents with new combinations of useful properties. New adsorbents and adsorption processes will be developed to provide needed improvements in pollution control, energy conservation, and the separation of high value chemicals. New process cycles and new hybrid processes linking adsorption with other unit operations will continue to be developed.

6.1. Fundamentals. Marked improvements in the prediction of multicomponent equilibrium from single-component data will be achieved by developing more realistic theoretical models that provide for nonideal adsorbate phases and heterogeneities of surface energetics and geometries, and that allow for the effect of adsorbates on adsorbent properties. Molecular modeling and molecular-dynamic simulations of adsorption phenomena on high speed computers will enable better prediction of multicomponent adsorption behavior and design of adsorbents with desired properties.

6.2. New Adsorbent Materials. Hydrophobic molecular sieves, mesoporous molecular sieves, macroreticular resins, and new carbon molecular sieves will continue to find new application. Carbon nanotubes and pillared interlayer clays (PILCS) will become more available for commercial applications, including adsorption. Adsorbents with enhanced performance, both highly selective physical adsorbents and easily regenerated, weak chemisorbents will be developed.

6.3. Process Concepts. More hybrid systems involving gas-phase adsorption coupled with catalytic processes and with other separations processes (especially distillation and membrane systems) will be developed to take advantage of the unique features of each. The roles of adsorption systems will be to efficiently achieve very high degrees of purification; to lower fouling contaminant concentrations to very low levels in front of membrane and other separations processes; or to provide unique separations of azeotropes, close-boiling isomers, and temperature-sensitive or reactive compounds.

6.4. Design Methods. Improvements in the ability to predict multicomponent equilibrium and mass-transfer rate performance will allow continued improvements in the design of new adsorption systems and in the energy efficiency of existing systems.

6.5. Computer Systems. Improved "smart" control systems based on new computer capabilities and control algorithms will be used increasingly in adsorption systems to provide more efficient operation. For example, the adjustment of the adsorption—regeneration cycle to account for changing feed compositions and flow rates can significantly reduce energy consumption by carrying out regenerations only when needed. Enhanced computer capabilities will also allow coupling of more sophisticated equilibrium models with more exact models for adsorption dynamics to provide improved design tools.

BIBLIOGRAPHY

"Adsorptive Separation, Gases" in *ECT* 3rd ed., Vol. 1, pp. 544–581, by D. B. Broughton, UOP Process Division, UOP Inc.; in *ECT* 4th ed., Vol. 1, pp. 529–573, by John D. Sherman and Carmen M. Yon, UOP; "Adsorption, Gas Separation" in *ECT* (online), posting date: December 4, 2000, by John D. Sherman, Carmen M. Yon, UOP.

CITED PUBLICATIONS

1. G. E. Keller, II, R. A. Anderson, and C. M. Yon, in R. W. Rousseau, ed., *Handbook of Separation Process Technology*, John Wiley & Sons, Inc., New York, 1987, pp. 644–696.
2. J. O. Hirschfelder, C. F. Curtiss, and R. B. Bird, *Molecular Theory of Gases and Liquids*, John Wiley & Sons, Inc., New York, 1954, pp. 215, 949, 1110.
3. R. M. Barrer and D. E. W. Vaughan, *J. Phys. Chem. Solids* **32**, 731 (1971).
4. R. M. Barrer, *Zeolites and Clay Minerals as Adsorbents and Catalysts*, Academic Press, London, 1978, pp. 164, 174, 185.
5. D. W. Breck and J. V. Smith, *Sci. Am.*, 8 (Jan. 1959).
6. *Data from Union Carbide Molecular Sieves*, UOP, Tarrytown, N.Y.
7. W. A. Steele, *Adv. Colloid Interface Sci.* **1**, 3 (1967). (Review with 360 refs.).
8. D. M. Ruthven, *Principles of Adsorption and Adsorption Processes*, John Wiley & Sons, Inc., New York, 1984, Chapts. 3, 4, p. 108.
9. W. Rudzinski, K. Nieszporek, H. Moon, and H-K Rhee, *Pol. Heterog. Chem. Rev.* **1**, 275 (1994) (in English); *Chem. Abstr.* **123**, 535166 (1995).
10. P. Selvam, S. K. Bhatia, and C. G. Sonwane, *Ind. Eng. Chem. Res.* **40**, 3237 (2001).
11. A. L. Myers, *NATO ASI Ser., Ser. E.* **158** (*Adsorpt. Sci. Technol.*), 15 (1989).
12. D. P. Valenzuela and A. L. Myers, *Adsorption Equilibrium Data Handbook*, Prentice Hall, Engelwood Cliffs, N.J., 1989.
13. D. P. Valenzuela and A. L. Myers, *Sep. Purif. Methods* **13**(2), 153 (1984).
14. O. Talu and A. L. Myers, *AIChE J.* **34**, 1887 (1988).
15. Y. K. Tovbin, *Langmuir* **13**, 979 (1997).
16. R. T. Yang, *Gas Separation by Adsorption Processes*, Butterworths, Boston, 1987, p. 86.
17. C. M. Yon and P. H. Turnock, *AIChE Symp. Ser.* **67**(117), 75 (1971).
18. R. T. Maurer, in J. R. Katzer, ed., *Molecular Sieves—II* (ACS Symp. Ser. 40) American Chemical Society, Washington, D.C., 1977, p. 379.
19. N. Sundaram, *Langmuir* **9**, 1568 (1993).
20. P. M. Mathias, R. Kumar, J. D. Moyer Jr., J. M. Schork, S. R. Srinivasan, S. R. Auvil, and O. Talu, *Ind. Eng. Chem. Res.* **35**, 2477 (1997).

21. R. T. Maurer, *AIChE J.* **43**, 388 (1997).
22. I. Langmuir, *J. Am. Chem. Soc.* **40**, 1361 (1918).
23. M. Volmer, *Z. Phys. Chem.* **115**, 253 (1925).
24. R. H. Fowler and E. A. Guggenheim, *Statistical Thermodynamics*, Cambridge University Press, Cambridge, 1939.
25. T. L. Hill, *Introduction to Statistical Thermodynamics*, Addison-Wesley, Reading, Mass., 1960.
26. V. A. Bakaev, *Dokl. Akad. Nauk SSSR* **167**, 369 (1967).
27. L. Riekert, *Adv. Catal.* **21**, 287 (1970).
28. P. Brauer, A. Lopatkin, and G. Ph. Stepanez, in E. M. Flanigen and L. B. Sand, eds., *Molecular Sieve Zeolites, Adv. in Chem 102*, American Chemical Society, Washington, D.C., 1971, p. 97.
29. D. M. Ruthven, K. F. Loughlin, and K. A. Holborrow, *Chem. Eng. Sci.* **28**, 701 (1973).
30. D. M. Ruthven, *Nat. Phys. Sci.* **232**(29), 10 (1971).
31. Ref. 8, p. 75ff.
32. M. M. Dubinin and L. V. Radushkevich, *Dokl. Akad. Nauk SSSR, Ser. Khim.* **55**, 331 (1947).
33. M. M. Dubinin and V. A. Astakhov, *Izv. Akad. Nauk. SSSR, Ser. Khim.* **71**, 5 (1971).
34. C. J. Radke and J. M. Prausnitz, *Ind. Eng. Chem. Fundam.* **11**, 445 (1972); *AIChE J.* **18**, 761 (1972).
35. J. Toth, *Acta. Chim. Acad. Sci. Hung.* **69**, 311 (1971).
36. S. Brunauer, P. H. Emmett, and E. Teller, *J. Am. Chem. Soc.* **60**, 309 (1938).
37. E. C. Markham and A. F. Benton, *J. Am. Chem. Soc.* **53**, 497 (1931).
38. R. Sips, *J. Chem. Phys.* **16**, 490 (1948).
39. A. L. Myers and J. M. Prausnitz, *AIChE J.* **11**, 121 (1965).
40. S. Suwanayuen and R. P. Danner, *AIChE J.* **26**, 68, 76 (1980).
41. T. W. Cochran, R. L. Kabel, and R. P. Danner, *AIChE J.* **31**, 268 (1985).
42. D. Nicholson and T. Stubos, *Membr. Sci. Technol. Ser.* **6**, 231 (2000); *Chem. Abstr.* **133**, 753508 (2000).
43. K. E. Gubbins, *NATO ASI Ser. Ser. C* **491**, 65 (1997); *Chem. Abstr.* **129**, 248956 (1998).
44. J. J. Low, J. D. Sherman, L. S. Cheng, R. L. Patton, A. Gupta and R. Q. Snurr, Paper Presented at the 7th International Conference on Fundamentals of Adsorption, Nagasaki, Japan, May 20–25, 2001.
45. G. M. Davies and N. A. Seaton, in F. Meunier, ed., *Fund. of Ads., Proc. VIth Int. Conf. of Fund. of Ads. (1998), LAS*, pp. 835–840 (1998).
46. R. L. Portsmouth and L. F. Gladden, *Chem. Eng. Res. Dev.* **70**, 186 (1992).
47. A. Kohl and F. Riesenfeld, *Gas Purification*, 4th ed., Gulf Publishing Co., Houston, Tex., 1985, p. 651.
48. K. S. W. Sing and co-workers, *Pure Appl. Chem.* **57**, 603 (1985).
49. D. W. Breck, *Zeolite Molecular Sieves—Structure, Chemistry, and Use*, John Wiley & Sons, Inc., New York, 1974.
50. R. C. Bansal, J.-B. Donnet, and F. Stoeckli, *Active Carbon*, Marcel Dekker, New York, 1988, p. ix.
51. E. M. Flanigen, J. M. Bennett, R. W. Grose, J. P. Cohen, R. L. Patton, R. M. Kirchner, and J. V. Smith, *Nature (London)* **271**, 512 (1978).
52. E. M. Flanigen and R. L. Patton, UOP, Tarrytown, N.Y., private communication.
53. R. C. Bansal, T. L. Dhami, and S. Parkash, *Carbon* **16**, 389 (1978).
54. W. K. Lewis, E. R. Gilliland, B. Chertow, and W. P. Cadogan, *Ind. Eng. Chem.* **42**, 1326 (1950).
55. D. Chen, H. P. Rebo, K. Moljord, and A Holmen, *Chem. Eng. Sci.* **51**, 2687 (1996).
56. D. W. Price and P. S. Schmidt, *J. Air Waste Mgmt. Ass.* **48**, 1135 (1998).

57. M. Lordgooei, M. J. Rood, and M. Rostam-Abadi, *Proc., 91st Annu. Meet.—Air Waste Manage. Assoc.*, WA47B02/1-12 (1998).
58. J. D. Snyder and J. G. Leesch, *Ind. Eng. Chem. Res.* **40**, 2925–2933 (2001).
59. S. Saysset, G. Grevillot, and A. S. Lamine, *Recents Prog. Genie Procedes* **13**, 389 (1999) (in English); *Chem. Abstr.* **135**, 399274 (2001).
60. D. Basmadjian, *Can. J. Chem. Eng.* **53**, 234 (1975).
61. G. M. Lukchis, *Chem. Eng.* **80**, (13), 111; (16), 83; (18), 83 (1973).
62. D. M. Ruthven, *Chem. Eng. Progr.* **84**, 42 (1988).
63. E. Van den Bulck, J. W. Mitchell, and S. A. Klein, *J. Heat Transfer* **108**, 684 (1986).
64. Y. Zhou, S. Y. Lee, and T. K. Ghosh, *Chem. Eng. Commun.* **169**, 57 (1998).
65. S. M. Reiwani and D. J. Moschandreas, *NTIS. Report No. PB87-114120/GAR* 1–96 (1986).
66. M. Buelow and A. Micke, in M. D. LeVan, ed., *Fund. of Ads., Proc. 5th Int. Conf. of Fund. of Ads.*, pp. 131–138 (1996).
67. A. Salden and G. Eigenberger, *Chem. Eng. Sci.* **56**, 1605 (2001).
68. M. Yates, J. Blanco, P. Avila, and M. P. Martin, *Micro. Meso. Mater.* **37**, 201 (2000).
69. Y. Mistsuma, Y. Ota, and T. Hirose, *J. Chem. Eng. Jpn.* **31**, 482 (1998).
70. C. C. Huang, F. C. Lin and F. C. Lu, *Sep. Sci. Tech.* **34**, 555 (1999).
71. K. Gadkaree, D. L. Hickman, and T. V. Johnson, Soc. Automot. Eng., [Spec. Publ] SP-1165 *(Aspects of Automotive Filtration)*, pp. 89–92 (1996).
72. H. Juentgen, *Carbon* **15**, 273 (1977).
73. J. R. Kiovsky, P. B. Koradia, and D. S. Hook, *Chem. Eng. Progr.* **72**, 98 (1976).
74. S. G. Deng and Y. S. Lin, *Ind. Eng. Chem. Res.* **34**, 4063 (1995).
75. M. S. A. Baksh and R. T. Yang, *AIChE J.* **38**, 1357 (1992).
76. E. S. Kikkinides and R. T. Yang, *Ind. Eng. Chem. Res.* **32**, 2365 (1993).
77. W. D. Lovett and F. T. Cunniff, *Chem. Eng. Progr.* **70**, 43 (1974).
78. A. Dyer, *An Introduction to Zeolite Molecular Sieves*, John Wiley & Sons, Inc., New York, 1988, pp. 102–105.
79. G. V. Baron, *Beig. Process Technol. Proc.* **11**(*Separation Technology*) pp. 201–20. (1994) (in English): *Chem. Abstr.* **121**, 582551 (1994).
80. R. V. Jasra, N. V. Choudary, and S. G. T. Bhat, *Sep. Sci. Technol.* **26**, 885 (1991).
81. S. Sircar, M. B. Rao, and T. C. Golden, *Stud. Surf. Sci. Catal.* **120A**, 395 (1999).
82. R. T. Cassidy and E. S. Holmes, *AIChE Symp. Ser.* **80**, 68 (1984).
83. P. Cen and R. T. Yang, *Ind. Eng. Chem. Fundam.* **25**, 758 (1986).
84. S. S. Suh and P. C. Wankat, *AIChE J.* **35**, 523 (1989).
85. R. T. Cassidy, in W. H. Flank, ed., *Adsorption and Ion Exchange with Synthetic Zeolites, Am. Chem. Soc. Symp. Ser. 135*, American Chemical Society, Washington, D.C., 1980, pp. 248–259.
86. G. E. Keller, II, in T. E. White, Jr., C. M. Yon, and E. H. Wagener, eds., *Industrial Gas Separations, Am. Chem. Soc. Symp. Ser. 223*, American Chemical Society, Washington, D.C., 1983, pp. 145–169.
87. C. W. Skarstrom, in N. N. Li, ed., *Recent Developments in Separation Science*, Vol. 2, CRC Press, Boca Raton, Fla., 1975, pp. 95–106.
88. J. W. Armond, in R. P. Townsend, ed., *The Properties and Applications of Zeolites*, The Chemical Society, London, 1980, pp. 92–102.
89. J. P. Ausikaitis in Ref. 18, pp. 681–695.
90. S. J. Collick, H. A. Johnson, and L. A. Robbins, *Environ. Prog.* **16**, 16 (1997).
91. M. Kawai and T. Kaneko, *Gas Sep. Purif.* **3**, 2 (1989).
92. T. C. Frankiewicz and R. G. Donnelly, in T. E. White, Jr., C. M. Yon, and E. H. Wagener, eds., *Industrial Gas Separations, Am. Chem. Soc. Symp. Ser. 223*, American Chemical Society, Washington, D.C., 1983, pp. 213–233.

93. E. Richter, *Erdoel Kohle, Erdgas, Petrochem.* **40**, 432 (1987).
94. A. Kapoor and R. T. Yang, *Chem. Eng. Sci.* **44**, 1723 (1989).
95. S. Sircar and R. Kumar, *Ind. Eng. Chem. Proc. Des. Dev.* **24**, 358 (1985).
96. R. T. Yang, *Gas Separation by Adsorption Processes*, Butterworths, Stoneham, Mass., 1987.
97. P. J. Clarke, J. E. Gerrard, C. W. Skarstrom, J. Vardi, and D. T. Wade, *SAE Trans.* **76**, 824 (1968).
98. Ref. 47, p. 421.
99. F. Adib, A. Bagreev, and T. J. Bandosz, *Ind. Eng. Chem. Res.* **39**, 2439 (2000).
100. A. Bagreev, H. Rahman, and T. J. Bandosz, *Carbon* **39**, 1319 (2001).
101. T. Y. Yan, *Ind. Eng. Chem. Res.* **33**, 3010 (1994).
102. J. T. Collins, M. J. Bell, and W. M. Hewitt, in A. A. Moghissi and co-workers, eds., *Nuclear Power Waste Technology*, American Society of Mechanical Engineers, New York, 1978, Chapt. 4.
103. D. W. Holladay, *A Literature Survey: Methods for the Removal of Iodine Species from Off-Gases and Liquid Waste Streams of Nuclear Power and Nuclear Fuel Reprocessing Plants, with Emphasis on Solid Sorbents*, Report ORNL/TM-6350 (Jan., 1979), p. 46, available from National Technical Information Service, Springfield, Va.
104. C. Berg, *Trans. Amer. Inst. Chem. Eng.* **42**, 665 (1946).
105. P. Cengiz, J. Abbasian, R. B. Slimane, K. K. Ho and N. R. Khalili, *Proc. Int. Tech. Conf. Coal Util. Fuel Syst. (2001), 26th*, pp. 893–897 (2001); Chem. Abstr. **135**, 517448 (2001).
106. E. S. Larsen and M. J. Pilat, *J. Air Waste Mgmt. Ass.* **41**, 1199 (1991).
107. J. M. Schork and J. R. Fair, *Ind. Eng. Chem. Res.* **27**, 457 (1988).
108. M. Leva, *Chem. Eng.* **56**, 115 (1949).
109. S. Sircar and A. L. Myers, *Ads. Sci. Technol.* **2**, 69 (1985).
110. M. S. Ray, *Sep. Sci. Tech.* **18**, 95 (1983).
111. M. Sakuth, A. Schweer, S. Sander, J. Meyer, and J. Gmehling, *Chem.-Ing.-Tech.* **70**, 1324 (1998) (in German).
112. M. S. Ray, *Stud. Surf. Sci. Catal.* **120A** (*Adsorption and Its Applications in Industry and Environmental Protection, Vol. 1*), pp. 977–1049 (1999).
113. D. M. Ruthven, *Ind. Eng. Chem. Res.* **39**, 2127 (2000).
114. K. Knaebel, D. Ruthven, J. L. Humphrey, R. Carr, J. R. Hufton, A. L. Myers, J. C. Crittenden and J. L. Bulloch, in P. P. Radecki, ed., *Emerging Sep. Sep. React. Technol. Process Waste Reduct*, American Institute of Chemical Engineers, New York, 1999, pp. 33–129.
115. A. Mersmann, A. , G. G. Borger, and S. Scholl, *Chem. Ing. Tech.* **63**, 892 (1991) (in German).
116. A. Dabrowski, in A. Dabrowski, ed., *Stud. Surf. Sci. Catal.* **120A**, 3 (1999).
117. M. S. Ray, *Ads. Sci. Tech.* **18**, 439 (2000).
118. E. Richter, W. Schutz and H. Juntgen, in A. B. Mersmann and co-workers, eds., *Fund. of Ads., Proc. 3rd Int. Conf. of Fund. of Ads.*, pp. 735–743 (1991).
119. S. J. Doong and R. T. Yang, *Ind. Eng. Chem. Res.* **27**, 630 (1988).
120. F. Karavias and A. L. Myers, *Langmuir* **7**, 3118 (1991).
121. G. Gamba, R. Rota, G. Storti, S. Carra, and M. Morbidelli, *AIChE J.* **35**, 959 (1989).
122. S. D. Mehta and R. P. Danner, *Ind. End. Chem. Fundam.* **24**, 325 (1985).
123. J. A. Ritter and R. T. Yang, *Ind. Eng. Chem. Res.* **26**, 1679 (1987).
124. R. Rota, G. Gamba, R. Paludetto, S. Carra, and M. Morbidelli, *Ind. Eng. Chem. Res.* **27**, 848 (1988).
125. M. Sakuth, J. Meyer, and J. Gmehling, *Chem. Eng. Proc.* **37**, 267 (1998).
126. G. Calleja, I. Pau, P. Perez, and J. A. Calles, in M. D. LeVan, ed., *Fund. of Ads., Proc. 5th Int. Conf. of Fund. of Ads.*, pp. 147–154 (1996).

127. J. Appel, *Surface Sci.* **39**, 237 (1973).
128. A. S. Michaels, *Ind. Eng. Chem.* **44**, 1922 (1952).
129. H. M. Barry, *Chem. Eng.* **67**, 105 (1960).
130. J. J. Collins, *Chem. Eng. Progr. Symp. Ser.* **63**, 31 (1967).
131. T. Vermeulen and G. Klein, *A.I.Ch.E. Symp. Ser.* **117**, 65 (1971).
132. A. Gorius, M. Bailly and D. Tondeur, *Chem. Eng. Sci.* **46**, 677 (1991).
133. S. Ramaswami, and C. Tien, *Ind. Eng. Chem. Proc. Des. Dev.* **25**, 133 (1986).
134. S. L. Forbes and D. W. Underhill, *JAPCA* **36**, 61 (1986).
135. R. Mohilla, J. Argelan, and R. Szolcsanyi, *Int. Chem. Eng.* **27**, 723 (1987).
136. D. Basmadjian and C. Karayannopoulos, *Ind. Eng. Chem. Proc. Des. Dev.* **24**, 140 (1985).
137. C. L. Humphries, *Hydrocarbon Process.* **45**, 88 (1966).
138. P. I. Cen and R. T. Yang, *AIChE J.* **32**, 1635 (1986).
139. H. Hori, I. Tanaka, and T. Akiyama, *JAPCA* **38**, 269 (1988).
140. H. Lee and W. P. Cummings, *Chem. Eng. Progr. Symp. Series* **63**(74), 42 (1967).
141. L. C. Eagleton and H. Bliss, *Chem. Eng. Progr.* **49**, 543 (1953).
142. J. W. Carter, *Br. Chem. Eng.* **14**, 303 (1969).
143. O. Grubner and W. A. Burgess, *Environ Sci. Technol.* **15**, 1346 (1981).
144. Y. E. Yoon and J. H. Nelson, *Am. Ind. Hyg. Assoc. J.* **45**, 517 (1984).
145. L. A. Jonas and J. A. Rehrmann, *Carbon* **11**, 59 (1973).
146. C. W. Chi and H. Lee, *AIChE Symp. Ser.* **69**, 95 (1973).
147. O. A. Hougen and W. K. Marshall, *Chem. Eng. Progr.* **43**, 197 (1947).
148. C. C. Furnas, *Trans. Am. Inst. Chem. Eng.* **24**, 142 (1930).
149. C. W. Chi, *AIChE Symp. Ser.* **74**, 42 (1977).
150. R. P. Underwood, *Chem. Eng. Sci.* **41**, 409 (1986).
151. R. Kumar and G. L. Dissinger, *Ind. Eng. Chem. Proc. Des. Dev.* **25**, 456 (1986).
152. I. Zwiebel, R. L. Gariepy, and J. J. Schnitzer, *AIChE J.* **18**, 1139 (1972); **20**, 915 (1974).
153. A. Jedrzejak and M. Paderewski, *Int. Chem. Eng.* **28**, 707 (1988).
154. J. L. Bravo, Report of DOE Contract No. DE-AS07-831D12473, 1984, pp. 150–181.
155. D. Basmadjian, K. D. Ha, and C. Y. Pan, *Ind. Eng. Chem. Proc. Des. Dev.* **14**, 328 (1975).
156. C. Huang and J. R. Fair, *AIChE J.* **35**, 1667 (1989).
157. M. M. Davis and M. D. LeVan, *Ind. Eng. Chem. Res.* **28**, 778 (1989).
158. A. Jedrzejak, *Chem. Eng. Technol.* **11**, 352 (1988).
159. D. H. White, Jr., and P. G. Barkley, *Chem. Eng. Progr.* **85**, 25 (1989).
160. K. Chihara and M. Suzuki, *J. Chem. Eng. Jpn.* **16**, 293 (1983).
161. J. W. Carter and M. L. Wyszynski, *Chem. Eng. Sci.* **38**, 1093 (1983).
162. R. Kumar, *Ind. Eng. Chem. Res.* **28**, 1677 (1989).
163. J. L. Liow and C. N. Kenney, *AIChE J.* **36**, 53 (1990).
164. H. Shin and K. S. Knaebel, *AIChE J.* **34**, 1409 (1988).
165. P. H. Turnock and R. H. Kadlec, *AIChE J.* **17**, 335 (1971).
166. S. J. Doong and R. T. Yang, *AIChE Symp. Ser.* **84**, 145 (1988).
167. S. Ergun, *Chem. Eng. Prog.* **48**, 89 (1952).
168. L. E. Brownell, H. S. Dombrowski, and C. A. Dickey, *Chem. Eng. Progr.* **46**, 415 (1950).

CARMEN M. YON
JOHN D. SHERMAN
UOP